

Competing phases of interacting electrons in twisted bilayer graphene and related moiré heterostructures

Michael M. Scherer

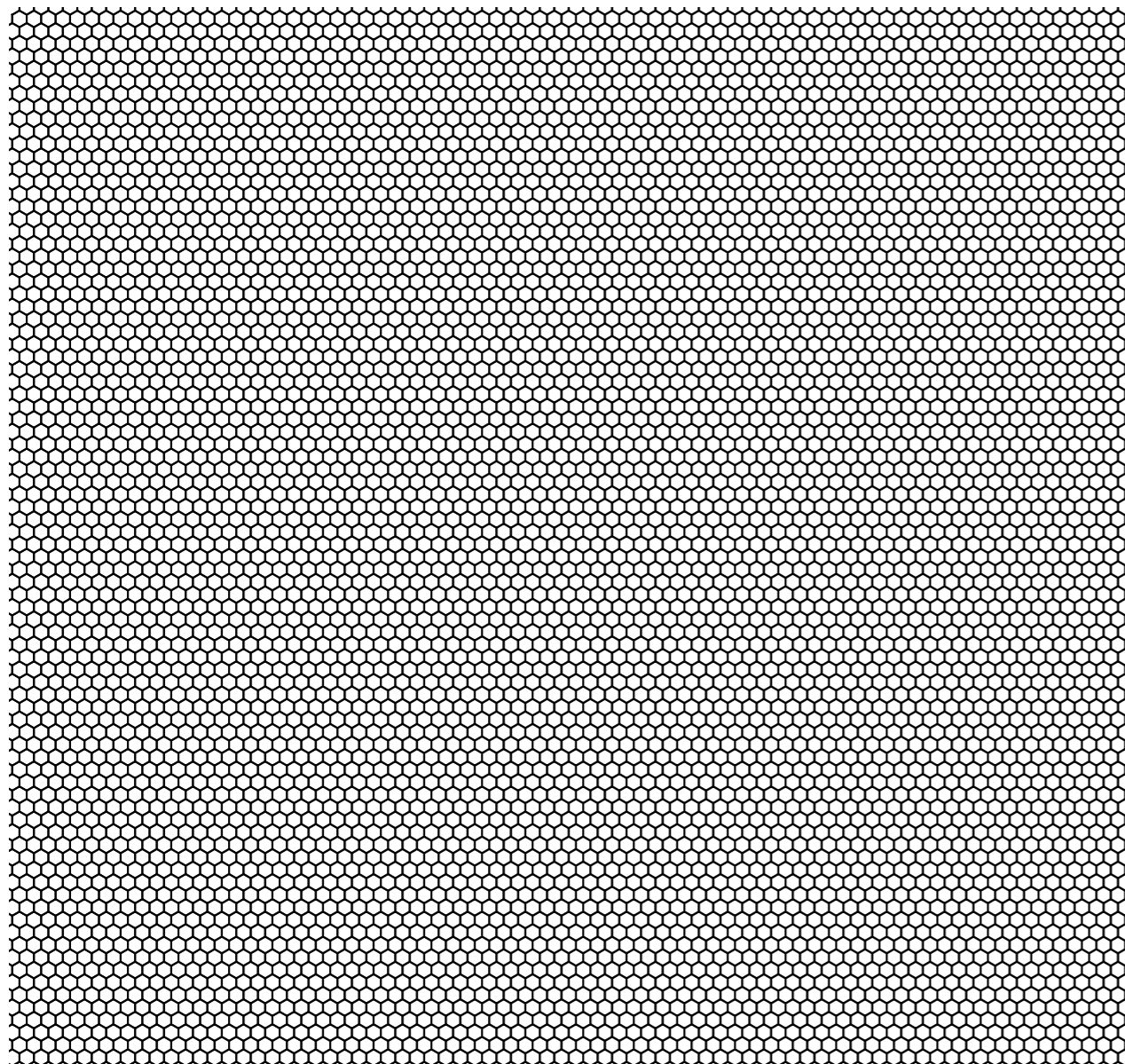
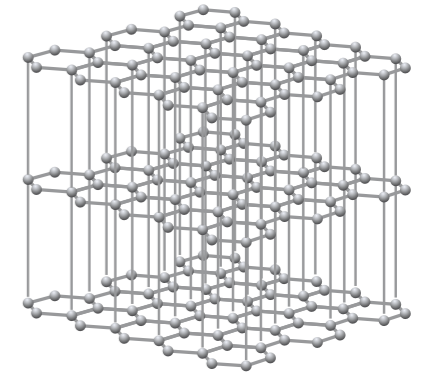
Institute for Theoretical Physics, Cologne University

June 26, 2019 @ Gießen University

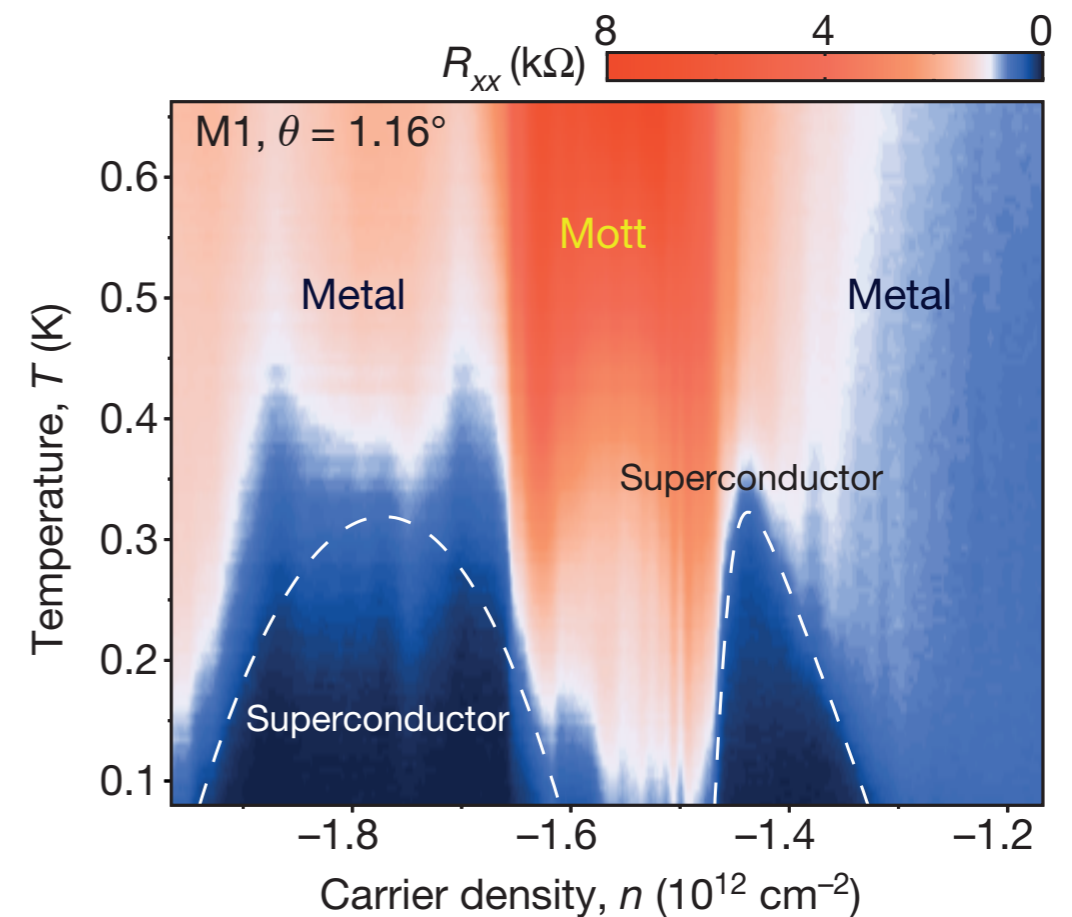
Magic-angle **twisted bilayer graphene**



- two graphene layers with small rotational mismatch θ
 - long-wavelength moiré pattern
 - @ $\theta_M \approx 1.05^\circ, 1.16^\circ$: $\sim 10,000$ atoms per moiré cell



- **correlated insulator and superconductivity**



- Cao et al., Nature 556, 43 (2018)
- Cao et al., Nature 556, 80 (2018) } **>900 citations**

Outline

- **Introduction & motivation**

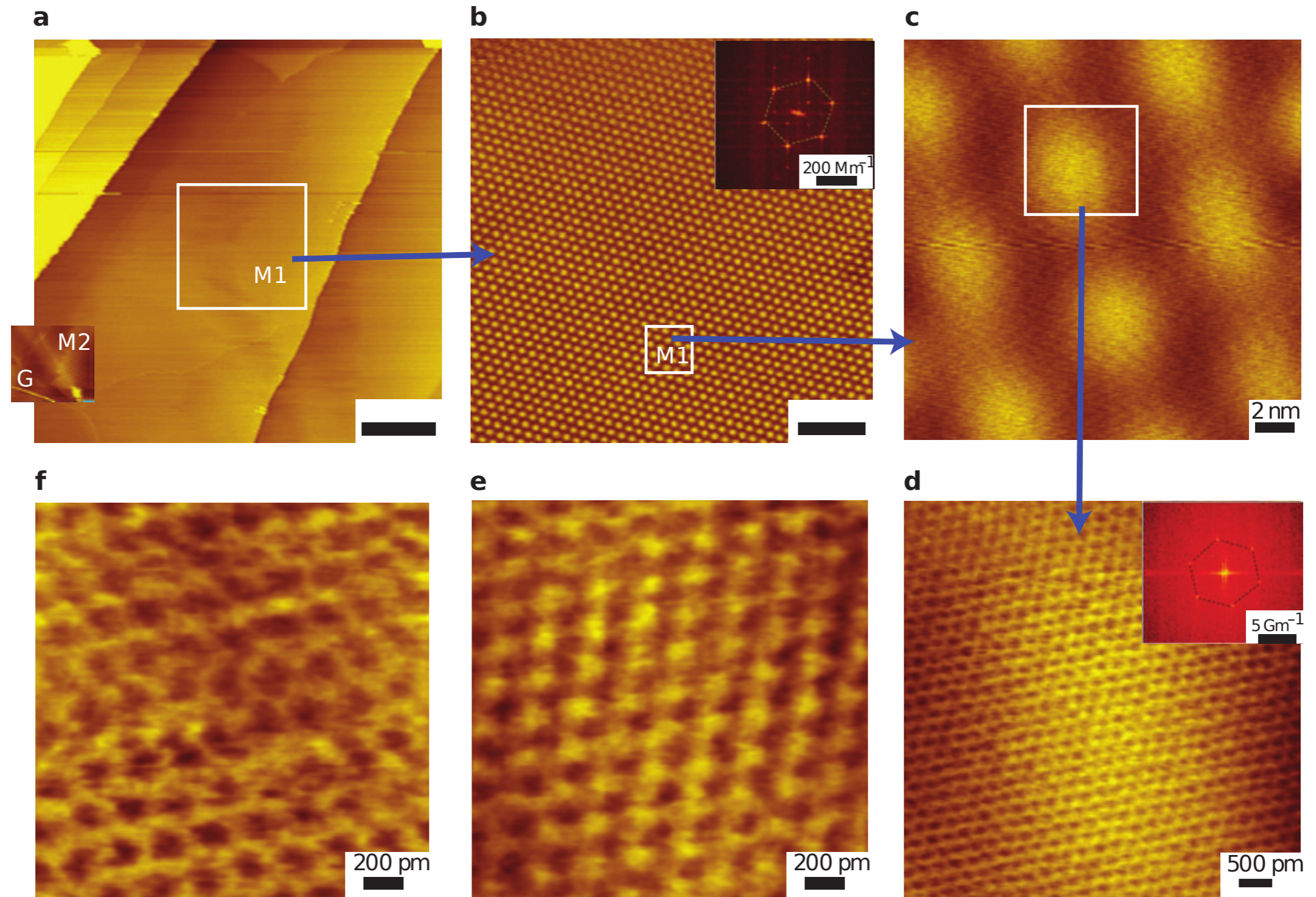
- twisted bilayer graphene - **basics & experiments**
- related moiré heterostructures
- twisted bilayer graphene - **models**

- **Effective lattice models & many-body approaches**

- **functional renormalization group** approach
- next-to-minimal model and tentative **phase diagram**
- conclusions & outlook

Twisted bilayer graphene - **basics & experiments**

Moiré pattern in STM



Correlated magic-angle **tBLG** - basic mechanism

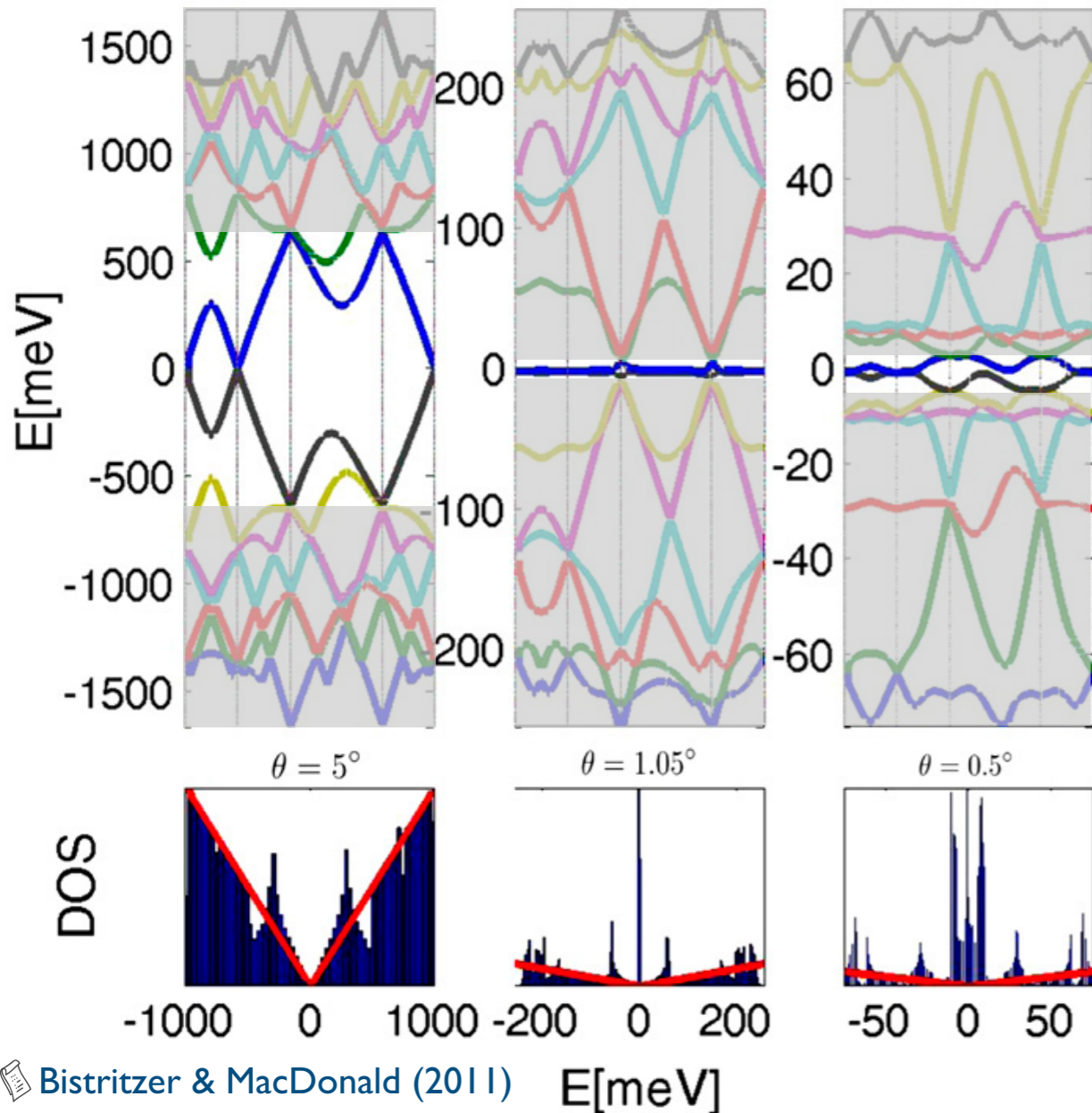
- for small twist angles $\theta < 10^\circ$

▸ moiré pattern \rightarrow superlattice potential \rightarrow *reconstruction of low-energy band structure:*

$\theta = 5^\circ$

$\theta = 1.05^\circ$

$\theta = 0.5^\circ$



- flat band structure at magic angle $\theta \approx 1^\circ$:

▸ $2 \times 2 \times 2 = 8$ nearly flat bands

- 2 bands crossing at mini-Dirac points

- spin (2 x)

- singlelayer valley (2 x)

▸ vary carrier concentration by gate voltage:

- between $n = \pm 4n_0$

(relative to charge neutrality)

- $n_0 \triangleq 1$ e⁻ per unit cell of superlattice

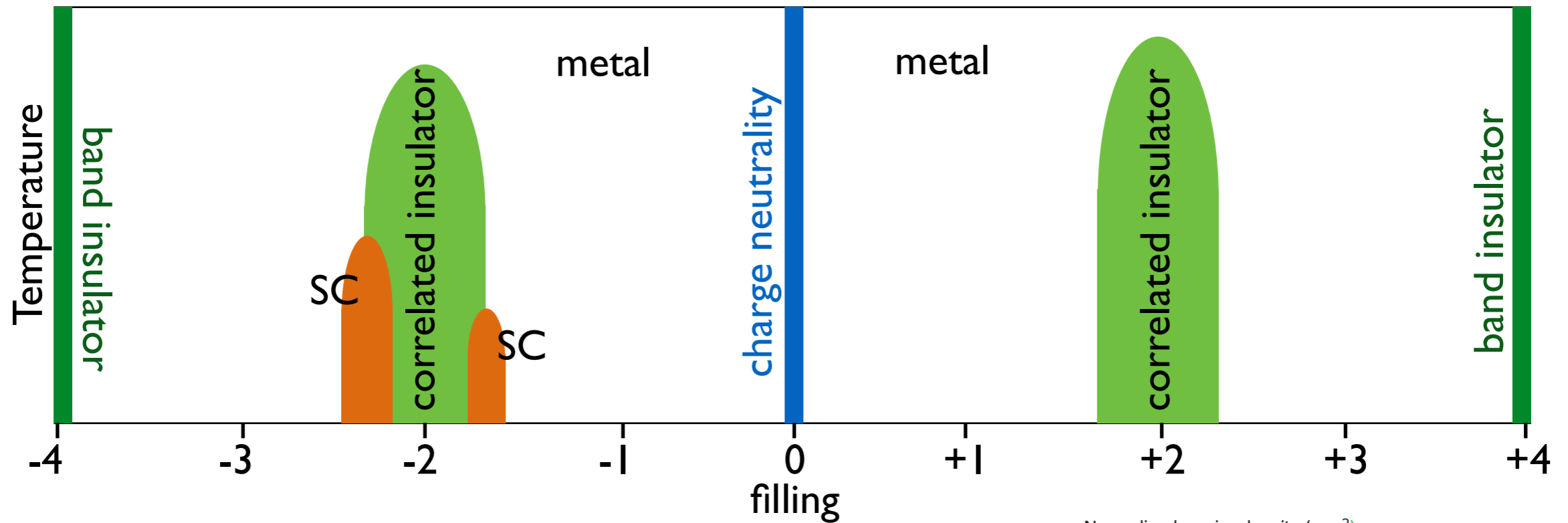


angle θ controls ratio bandwidth/interaction: $t/U \sim |\theta - \theta_M|$



strongly-correlated states!

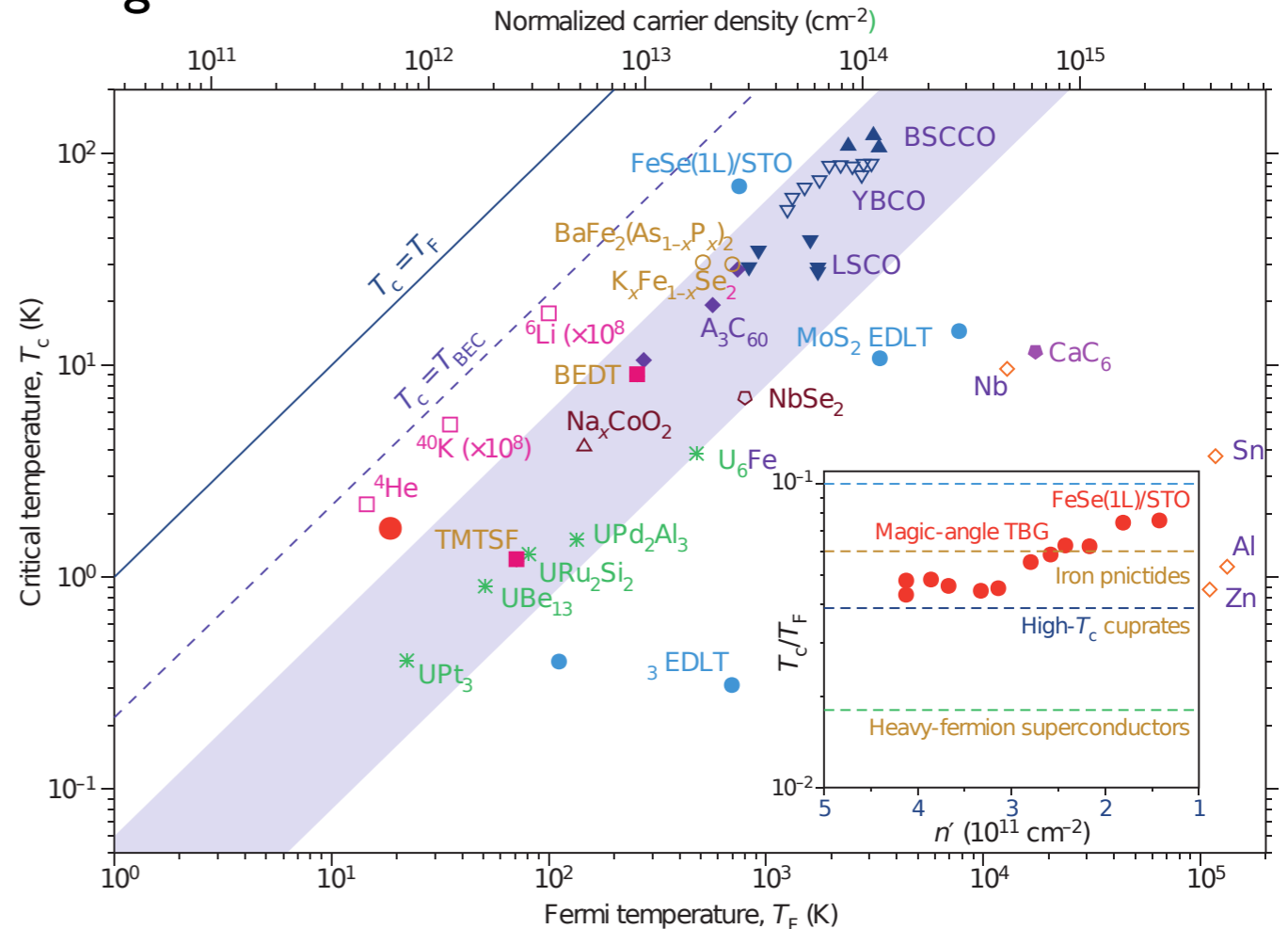
Magic-angle **tBLG** - phase diagram 1.0 (2018)



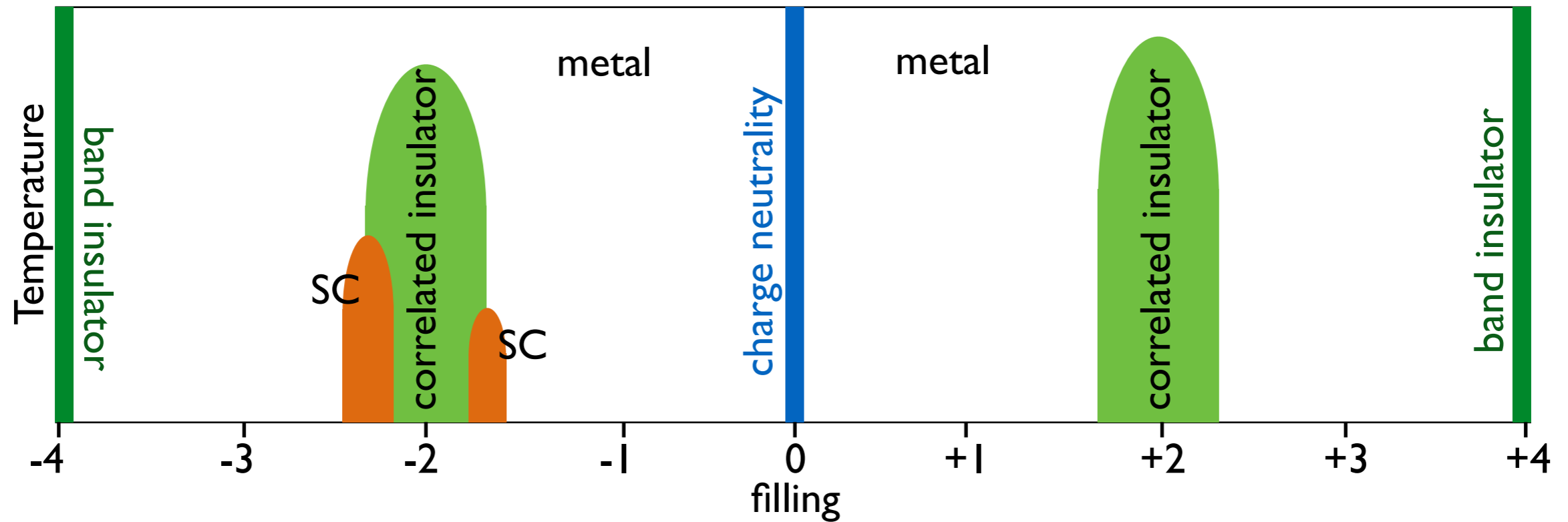
- *band insulator* at $n = \pm 4n_0$
- *correlated insulator* at $n = \pm 2n_0$
- *superconducting domes* at $n/n_0 = -2 \pm \delta$
 - $T_c \sim 1.7\text{K}$
 - T_c/T_F large
- resemblance to cuprate phase diagram!

Cao et al., Nature 556, 43 (2018)

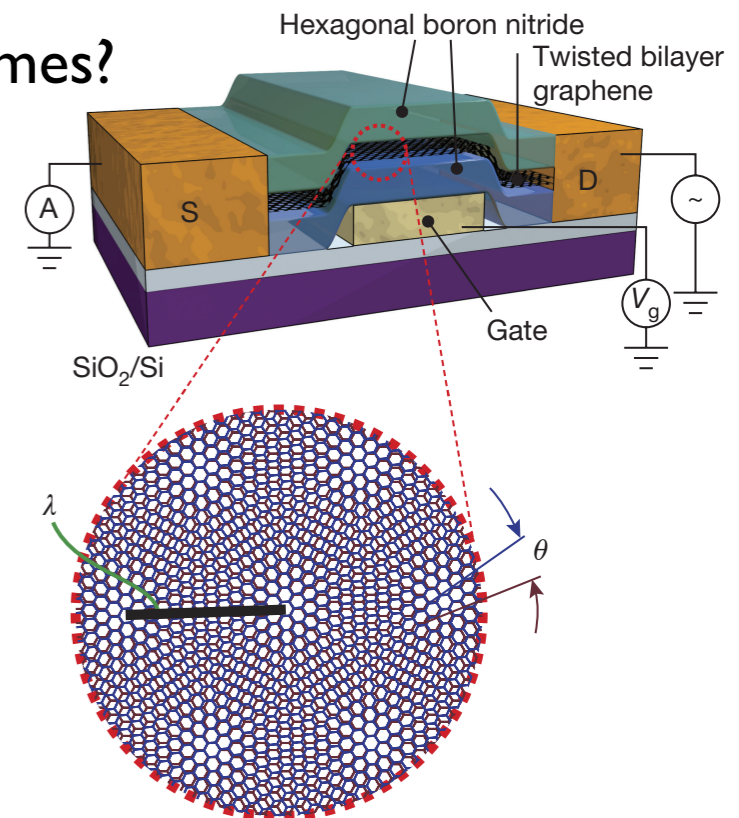
Cao et al., Nature 556, 80 (2018)



Questions

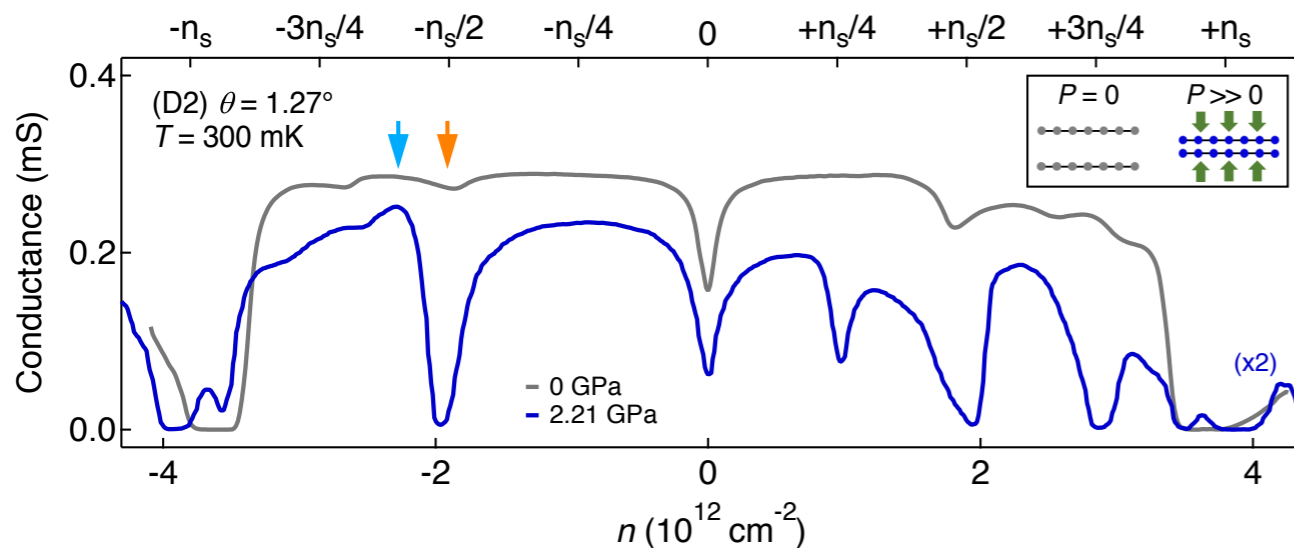


- Are the integer fillings $n/n_0 = \pm 2$ special?
- Are there *further correlated states* in different parameter regimes?
- Which *symmetries* are broken/preserved in correlated states?
 - spin-rotation / time-reversal / ... ?
- What is the *pairing channel* of the superconducting state?
- What is the role of *electron-phonon interactions*?
- How does the phenomenology depend on the *substrate*?



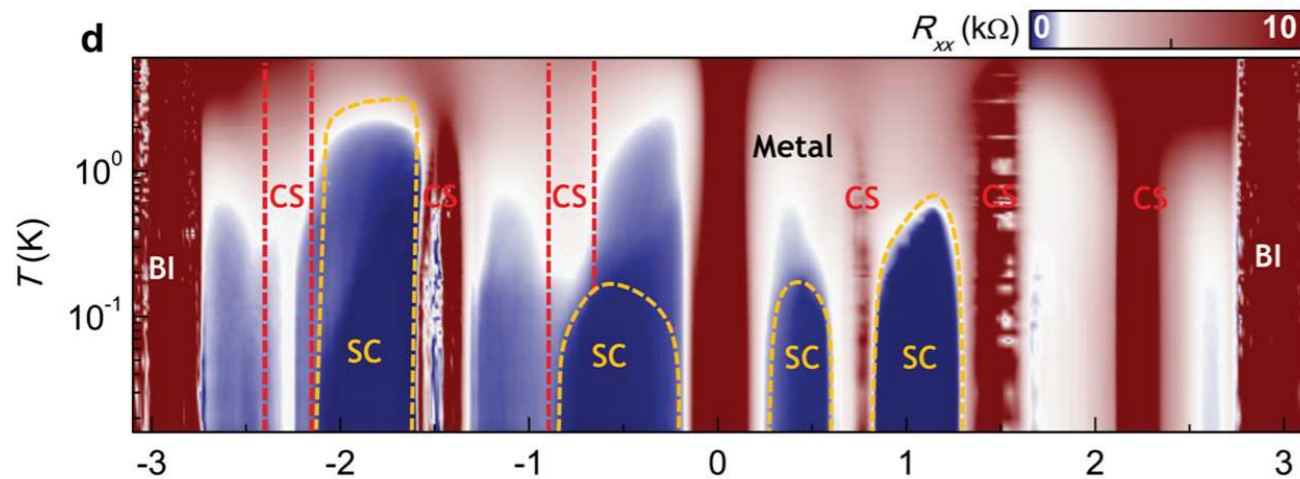
2nd generation of tBLG experiments (2019)

Columbia University: Yankowitz et al., Science 363, 1059 (2019)



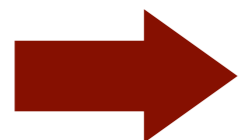
▶ correlated insulator also at $n/n_0 = +3$, superconductor near $n/n_0 = \pm 2$

Efetov Lab, Barcelona: Lu et al., arXiv:1903.06513



• more results on finite B_{\perp} , role of topology with aligned hBN substrate, Landau fans

Stanford: Sharpe et al., arXiv:1901.03520









new platform established for study of correlated electrons

✓ high control of twist angle, low level of disorder, pressure/gate tunable band widths/fillings

- *apply* hydrostatic *pressure* P
 - ➔ variation of interlayer tunneling w
 - ➔ changes magic angle $\theta_M \sim w$
 - ➔ in-situ control of $t/U \sim |\theta - \theta_M|$
- *pressure increases* θ_M
 - ➔ reduce moiré lattice constant
 - ➔ increase energy scale: $T_{c,SC} \sim 3K$

- *very low twist-angle disorder*
 - ▶ reduced modulations of θ across device
 - ▶ $\Delta\theta < 0.02^\circ$
 - ▶ insulating gaps at $n/n_0 = -3, -2, -1, 0, +1, +2, +3$
 - ▶ SC domes in between ($T_{c,SC} \sim 0.14 - 3K$)

Related 2D van der Waals **moiré** heterostructures

- *magic-angle twisted bilayer graphene* ✓
- *ABC trilayer graphene on hexagonal boron nitride*
 - **experiments:** tunable insulating and SC behavior
 -  Chen et al., Nat. Phys. 15, 237 (2019)
 -  Chen et al., arXiv:1901.04621 (2019)
- *twisted double bilayer graphene*
 - **experiments:** spin-polarized correlated insulating and SC behavior
 -  Liu et al., arXiv:1903.08130 (2019)
 -  Cao et al., arXiv:1903.08596 (2019)
- *twisted bilayer boron nitride*
 - **theoretical:** multi-flat bands and strong correlations
 -  Xian et al., arXiv:1812.08097 (2018)
- *transition metal dichalcogenides*
 - **theoretical:** flat bands and strong correlations with and without twist...
 -  Wu et al., PRL 121, 026402 (2018)

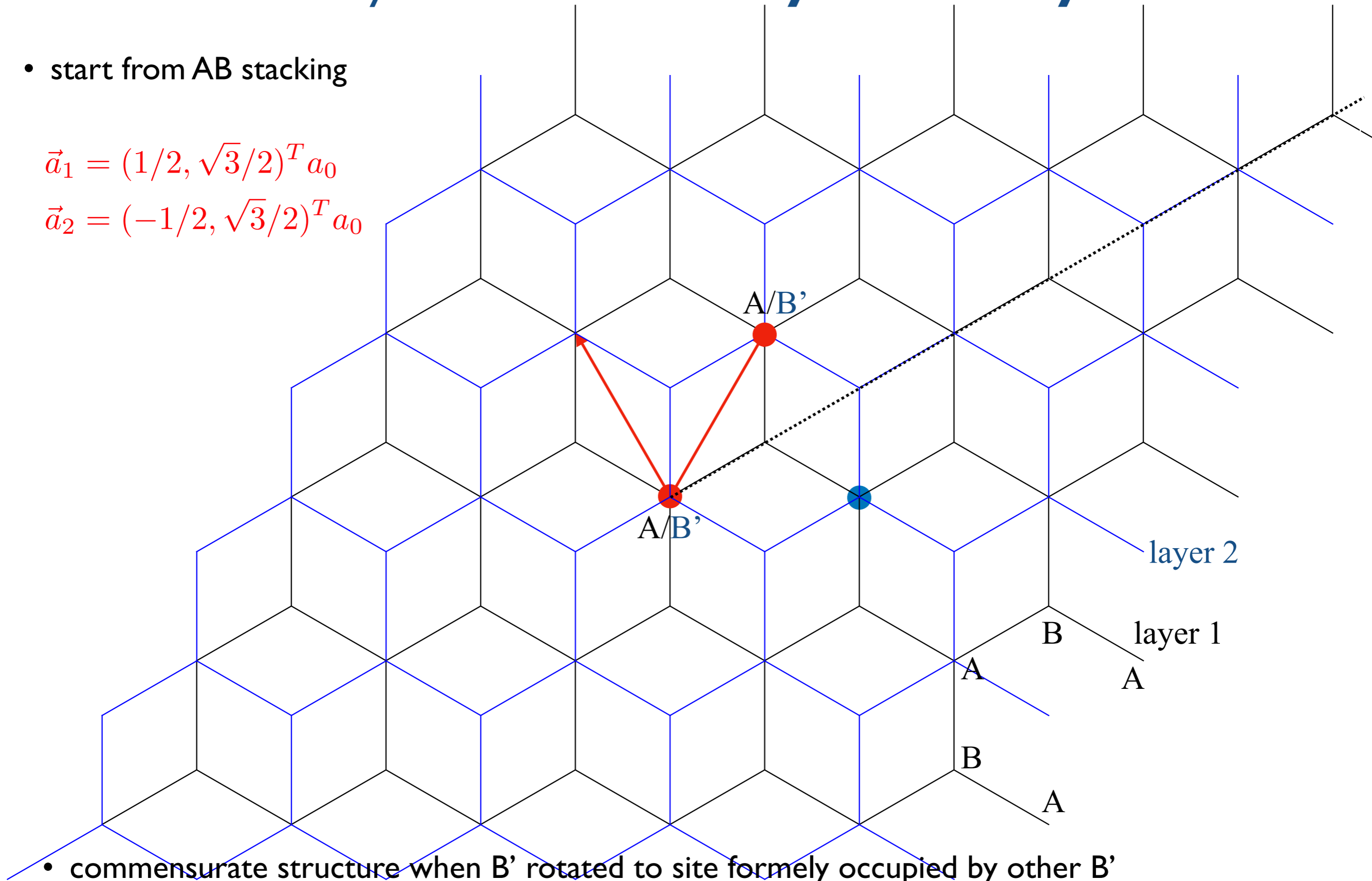
Twisted bilayer graphene - **models**

Geometry of **twisted honeycomb bilayers**

- start from AB stacking

$$\vec{a}_1 = (1/2, \sqrt{3}/2)^T a_0$$

$$\vec{a}_2 = (-1/2, \sqrt{3}/2)^T a_0$$



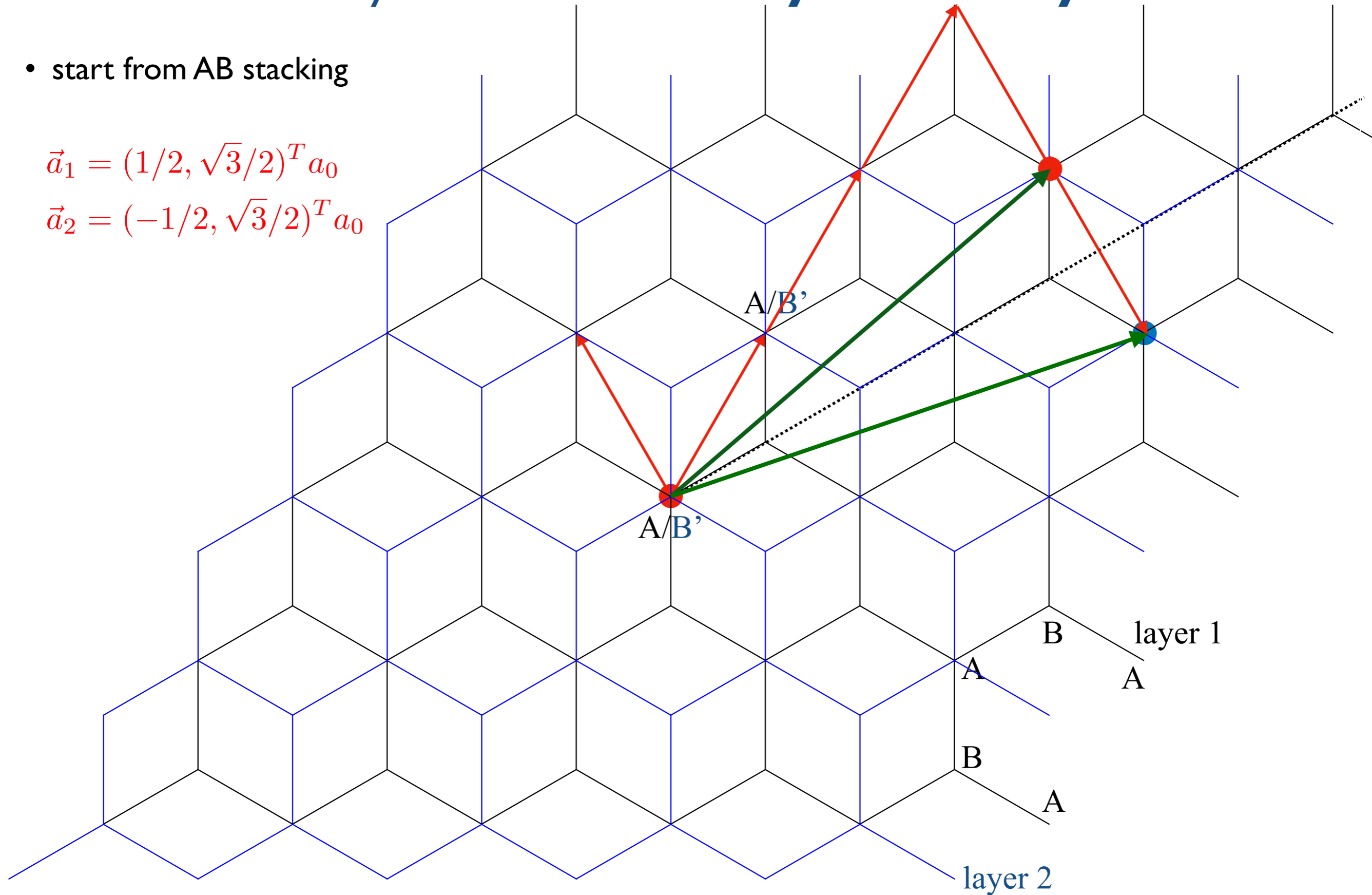
- commensurate structure when B' rotated to site formerly occupied by other B'
- 2D bilayer crystal only at discrete set of commensurate rotation angles

Geometry of **twisted honeycomb bilayers**

- start from AB stacking

$$\vec{a}_1 = (1/2, \sqrt{3}/2)^T a_0$$

$$\vec{a}_2 = (-1/2, \sqrt{3}/2)^T a_0$$

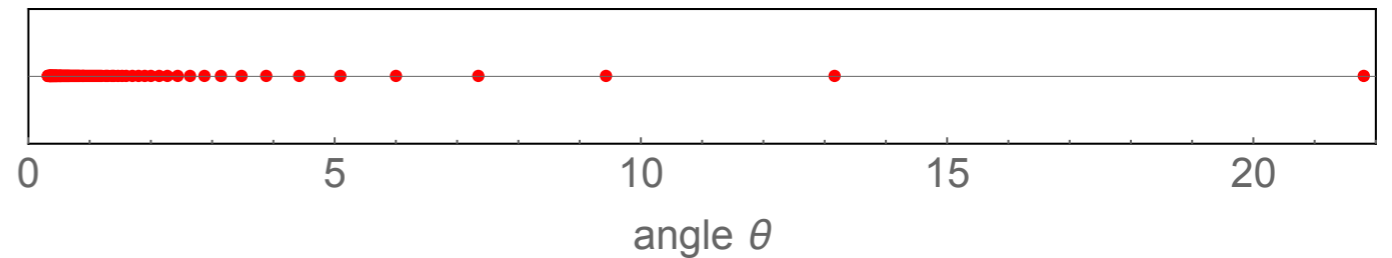


here: $\theta \approx 21.8^\circ$

Geometry of **twisted honeycomb bilayers**

- 2D bilayer crystal only at discrete set of commensurate rotation angles

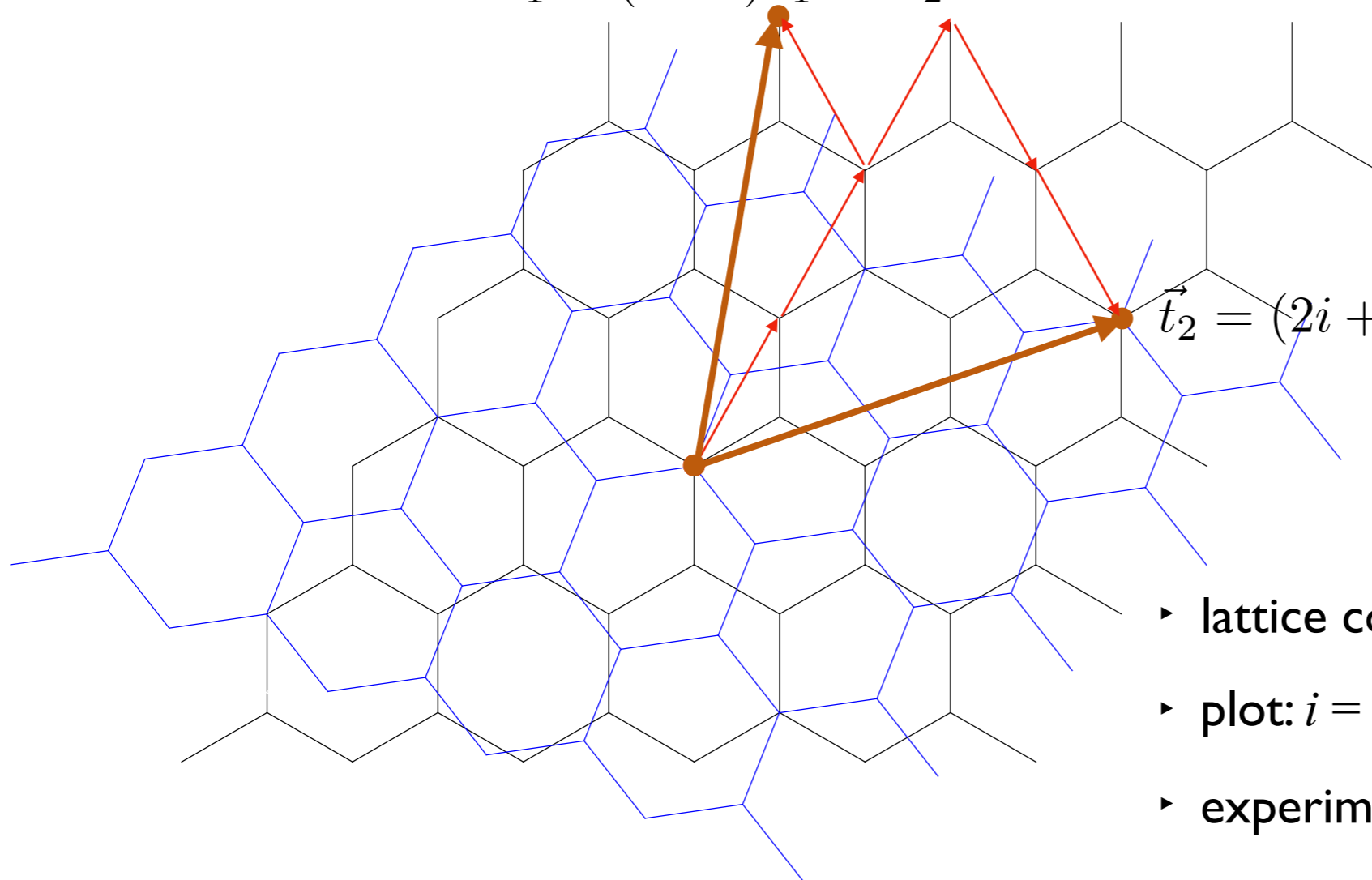
$$\cos(\theta_i) = \frac{3i^2 + 3i + 1/2}{3i^2 + 3i + 1}, \quad i \in \mathbb{N}_0$$



- emergent moiré superlattice spanned by real space lattice vectors t_1 and t_2

$$\vec{t}_1 = (i + 1)\vec{a}_1 + i\vec{a}_2$$

$$\vec{t}_2 = (2i + 1)\vec{a}_1 - (i + 1)\vec{a}_2$$



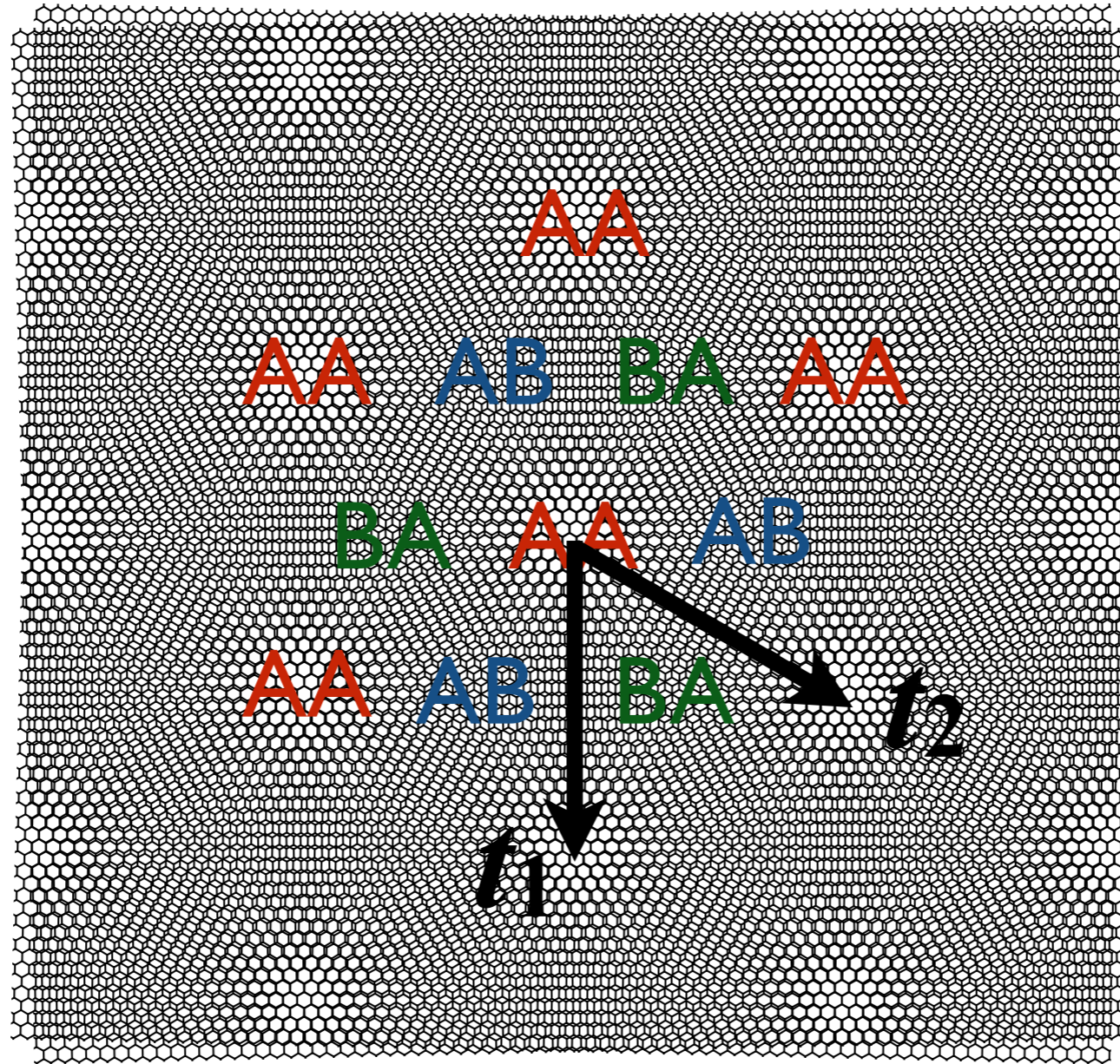
▸ lattice constant: $|\vec{t}_1| = \sqrt{3i^2 + 3i + 1}a_0$

▸ plot: $i = 1$

▸ experiment: $i \approx 30$

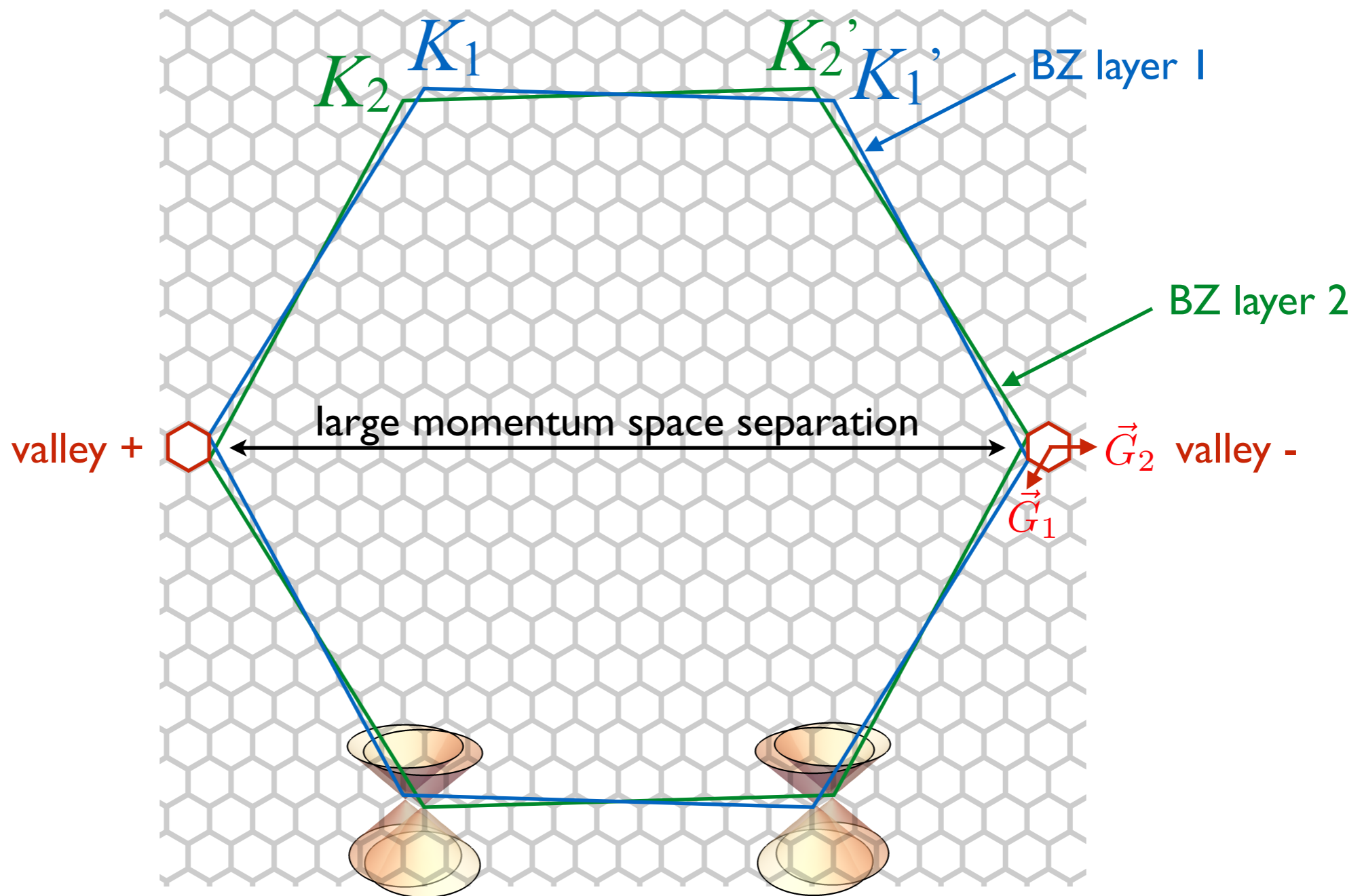
Geometry of **twisted honeycomb bilayers**

- example: $\theta \approx 2.6^\circ$ ($i = 12$)



- local AA, AB and BA stacking regions
- moiré superlattice vectors t_1 and t_2

Mini Brillouin zone



- reciprocal lattice vectors:

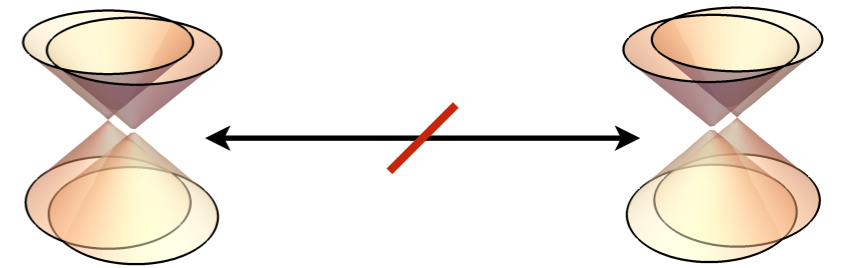
$$\vec{G}_1 = \frac{4\pi}{3(3i^2 + 3i + 1)} [\vec{a}_1 + (3i + 1)\vec{a}_2]$$

$$\vec{G}_2 = \frac{4\pi}{3(3i^2 + 3i + 1)} [(3i + 1)\vec{a}_1 - (3i + 2)\vec{a}_2]$$
- Dirac points of single-layer graphene layers: K_1, K_1', K_2, K_2'

Effective continuum model

- moiré period much larger than atomic scale → *continuum model*
- neglect intervalley mixing (large momentum space separation)

Lopes dos Santos et al., PRL 99, 256802 (2007)
 Bistritzer, MacDonald, PNAS 108, 12233 (2011)



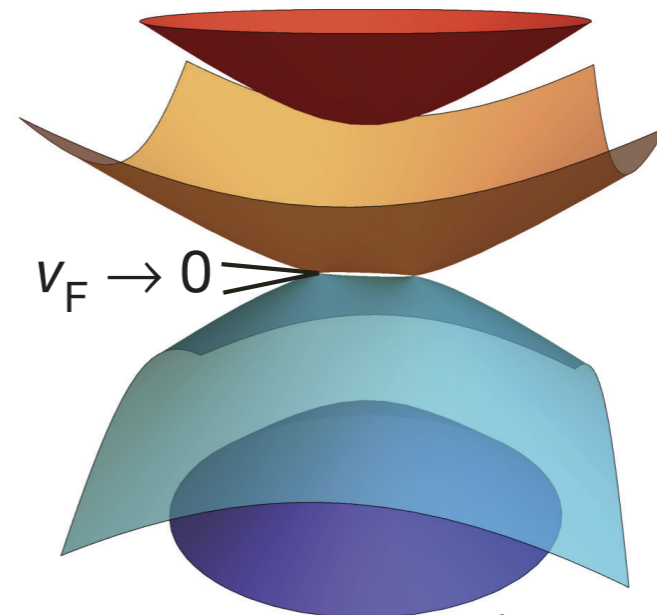
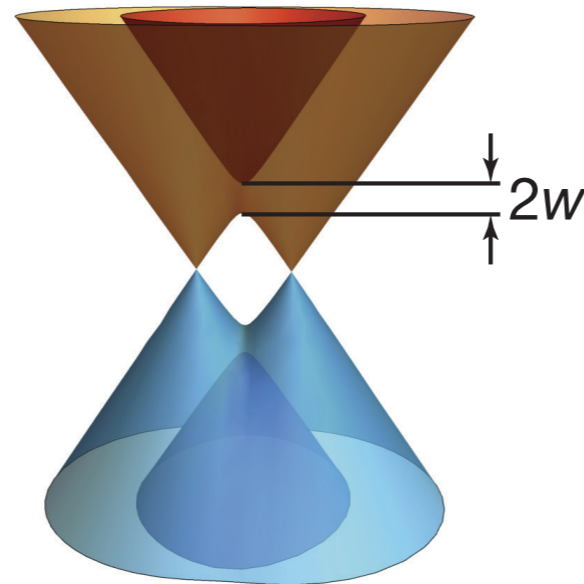
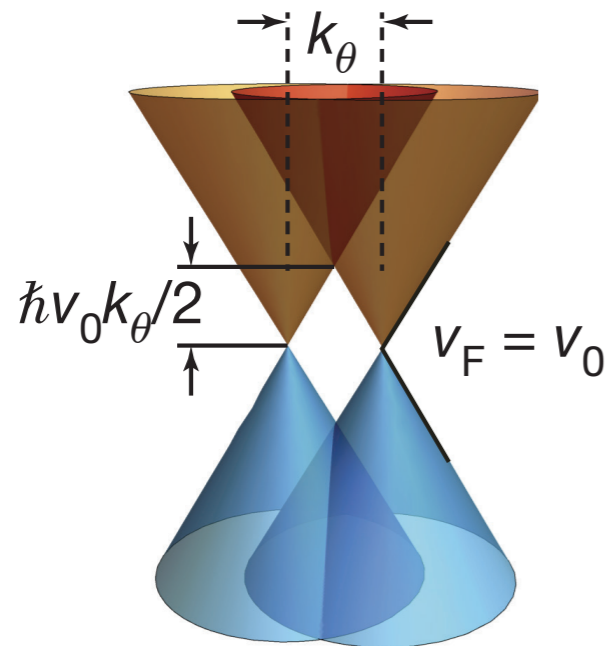
▸ independent calculation for each valley $\xi \in \pm$

▸ 1 Dirac cone from each layer: **interlayer hybridization**

▸ **effective 4x4 Hamiltonian**

$$H^{(\xi)} = \begin{pmatrix} H_1 & U^\dagger \\ U & H_2 \end{pmatrix}$$

intralayer Dirac Hamiltonians
 effective interlayer coupling



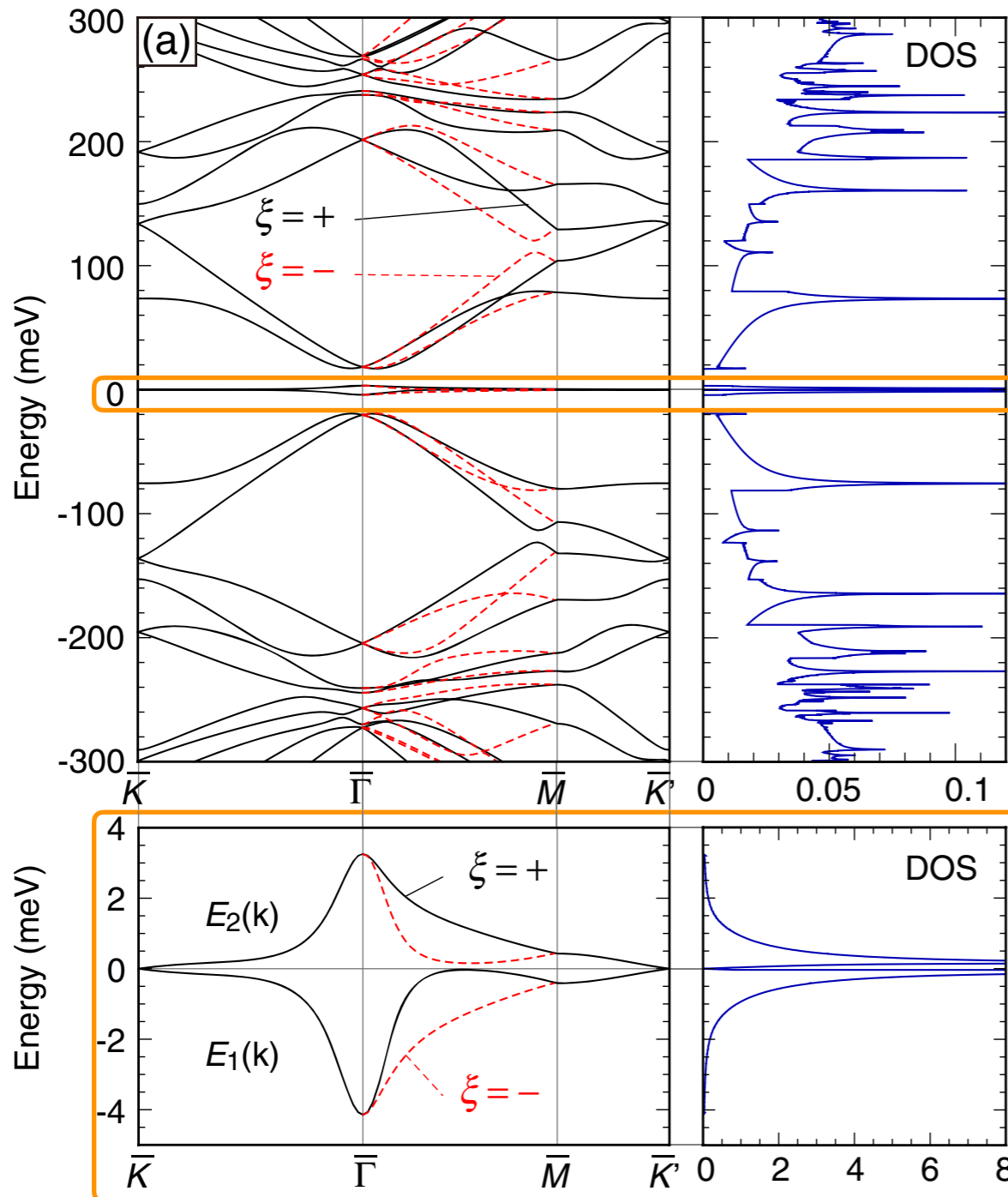
Cao et al, Nature 556, 80 (2018)

▸ Dirac cones become nearly flat for **magic angles**

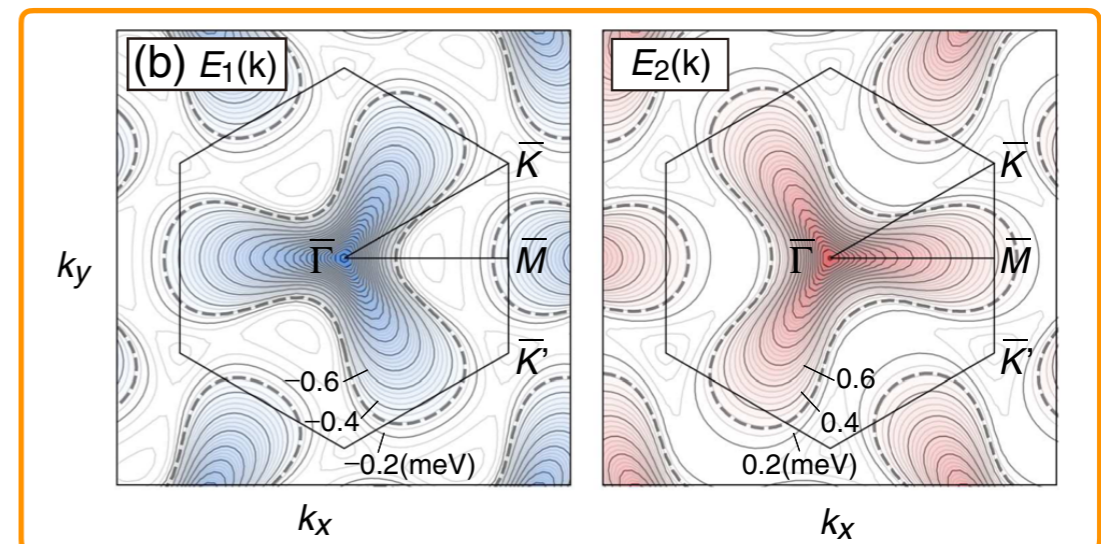
▸ dependence on modelling of interlayer coupling (*lattice relaxation, corrugation,...*)

Effective continuum model

- full calculation of band dispersion in continuum model

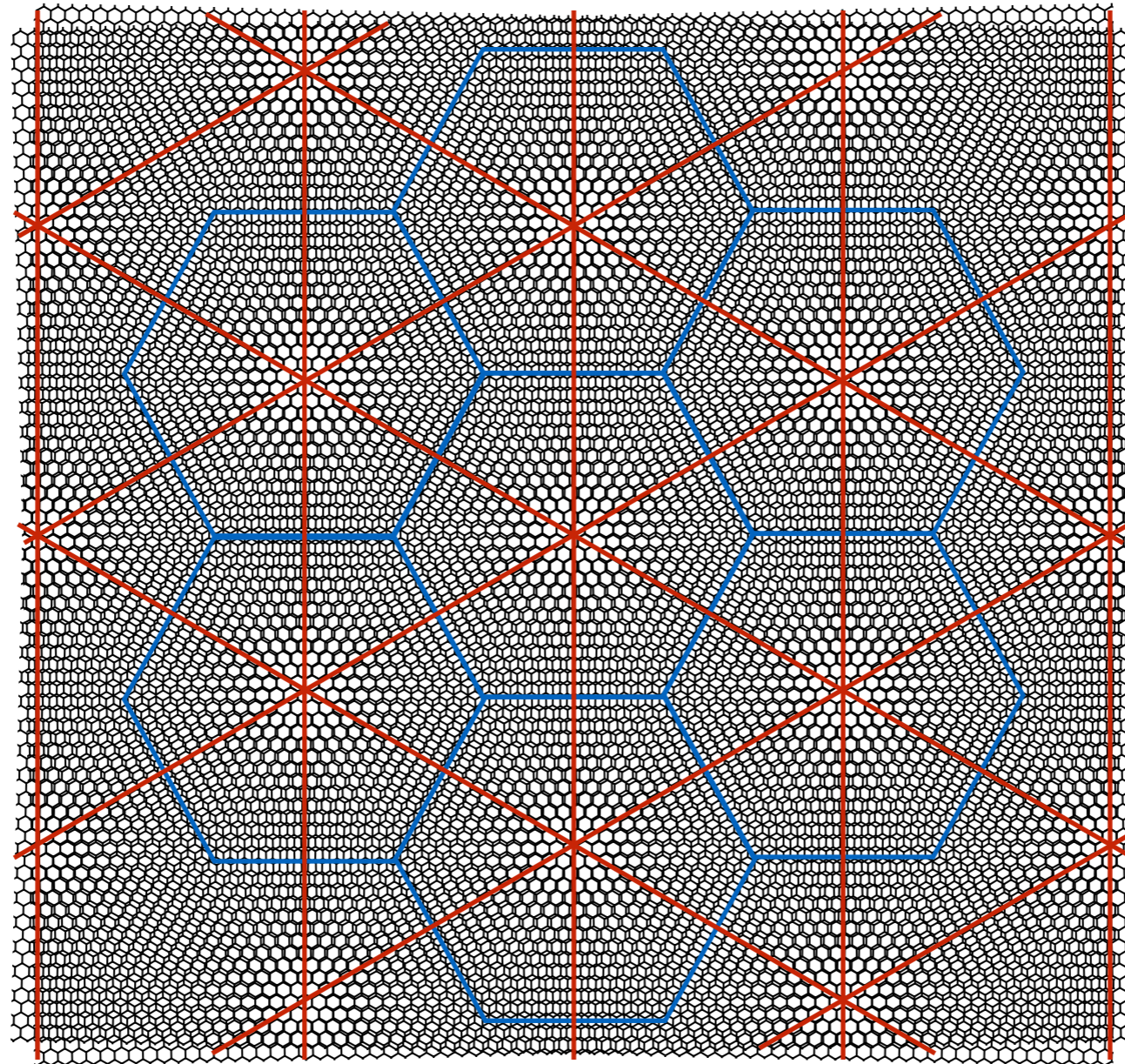


- at *magic angles* θ_M (here: $\theta_M = 1.05^\circ$)
 - emergence of multiple nearly flat bands
 - well-separated from other bands
 - van Hove singularities in flat bands



Wannier orbitals for flat bands & effective lattice model

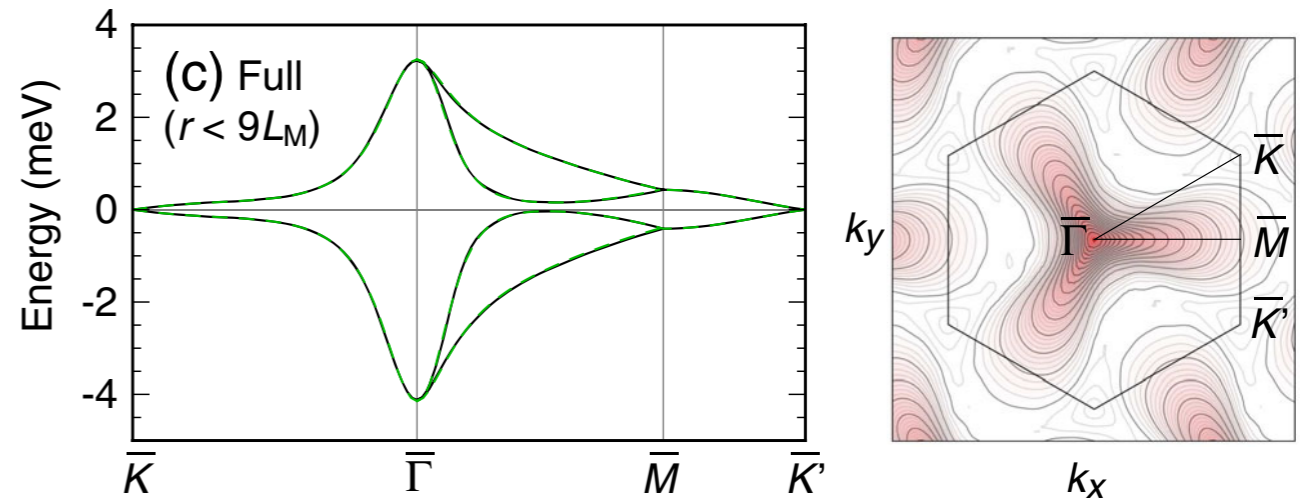
- *symmetry analysis* for tBLG:
 - Wannier orbitals centered at nonequivalent AB and BA spots in moiré pattern
 - formation of emergent honeycomb lattice



- emergent *triangular* lattice: ABC trilayer graphene-hBN, twisted double BLG, TMDs

Wannier orbitals for flat bands & effective lattice model

- flat band dispersion from continuum model
 - construct max-localized Wannier orbitals
 - tight-binding + extended Hubbard model

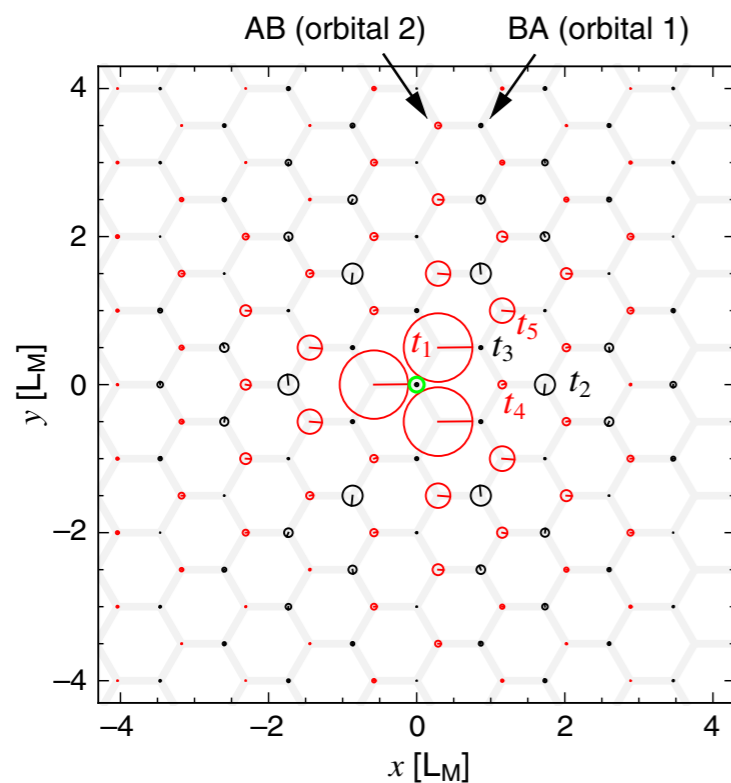


$$H = \sum_{\xi=\pm} \sum_{ij} t(\mathbf{r}_{ij}) e^{i\xi\phi(\mathbf{r}_{ij})} c_{i\xi}^\dagger c_{j\xi} + \text{extended Hubbard i.a.}$$

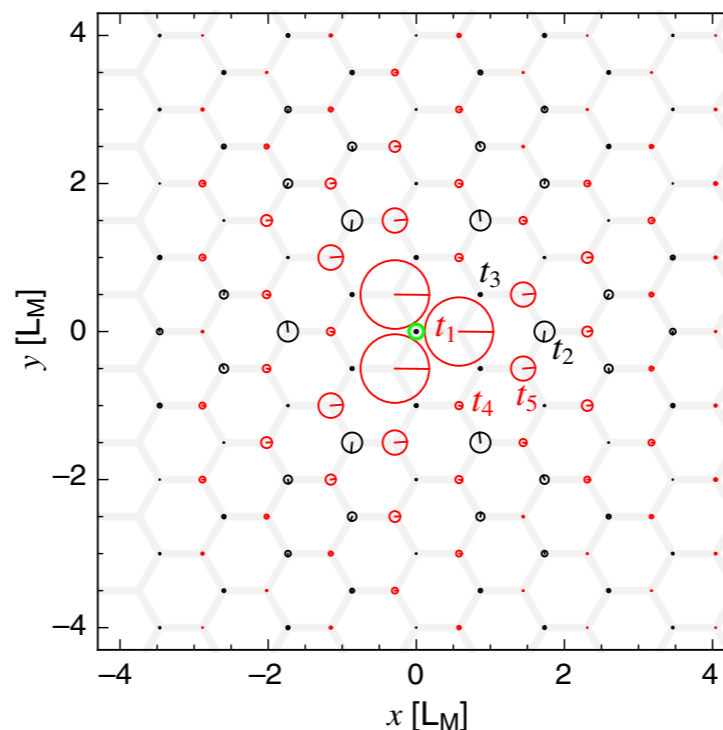
- hopping integrals and electron-electron interaction parameters:

[Koshino et al, PRX 8, 031087 \(2018\)](#)
[Kang & Vafeek, PRX 8, 031088 \(2018\)](#)

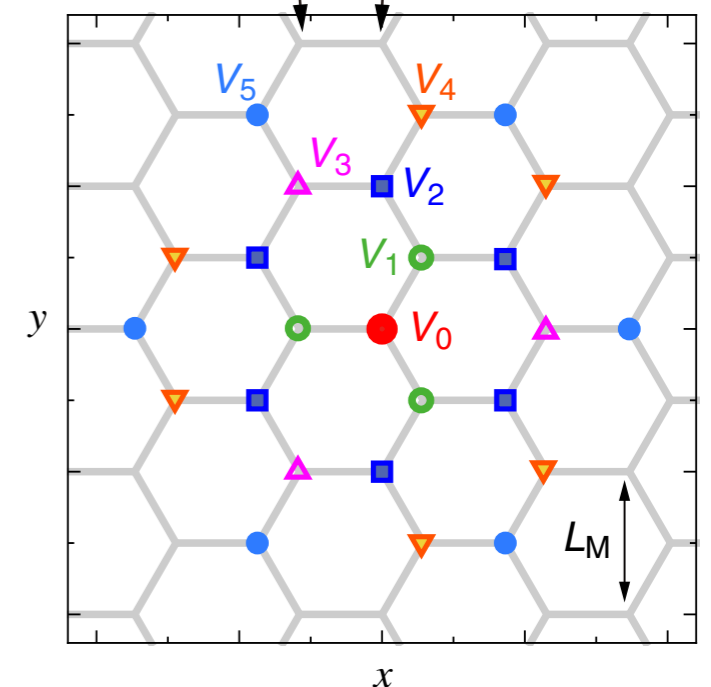
(a) From orbital 1



(b) From orbital 2



(a) AB (orbital 2) BA (orbital 1)



Correlated moiré heterostructures - **precis**

Precis

- 2D moiré heterostructures:

- emergent flat bands, **small kinetic energy**
- **enhanced interaction effects**



correlation-driven states!

- construction of effective models on emergent moiré honeycomb/triangular superlattice

- **universal features:**

- **multi-orbital** structure inherited from two valleys → **Hund's couplings**
- onsite and sizable **further-neighbor interactions**

*...starting point for application of **many-body methods...***

- **what is the nature of the correlated insulating and SC states?**

- Kekulé valence bond solid, (anti)ferromagnet, interaction-induced top. states, ...?
- featureless Mott insulator?
- gapped quantum spin liquid with neutral spin-1/2 excitations?
- topological/chiral d+id superconductor, f-wave superconductor, ...?

Functional **renormalization group approach**

Effective action

- ▶ system of interacting fermions: $\mathcal{S}[\psi, \bar{\psi}] = -(\bar{\psi}, G_0^{-1} \psi) + V[\psi, \bar{\psi}]$
general two-particle i.a.

- ▶ bare propagator (translation and spin rotation invariance):

$$G_0(k_0, \mathbf{k}) = \frac{1}{ik_0 - \xi_{\mathbf{k}}}, \quad \xi_{\mathbf{k}} = \epsilon_{\mathbf{k}} - \mu$$

single-particle energy

- ▶ generating functional (for connected Green functions):

$$\mathcal{G}[\eta, \bar{\eta}] = -\ln \int \mathcal{D}\psi \mathcal{D}\bar{\psi} e^{\mathcal{S}[\psi, \bar{\psi}]} e^{(\bar{\eta}, \psi) + (\bar{\psi}, \eta)}$$

- ▶ effective action: $\Gamma[\phi, \bar{\phi}] = (\bar{\eta}, \phi) + (\bar{\phi}, \eta) + \mathcal{G}[\eta, \bar{\eta}], \quad \phi = -\frac{\partial \mathcal{G}}{\partial \bar{\eta}}, \quad \bar{\phi} = \frac{\partial \mathcal{G}}{\partial \eta}$

(generates one-particle irreducible vertex functions)

Functional flow equations

- ▶ modify bare propagator by introduction of flow parameter


(IR cutoff, cuts out soft modes $< \Lambda$):
$$G_0^\Lambda(k_0, \mathbf{k}) = \frac{\Theta_\epsilon(|\xi_{\mathbf{k}}| - \Lambda)}{ik_0 - \xi_{\mathbf{k}}}$$

- ▶ define all the above quantities with modified bare propagator

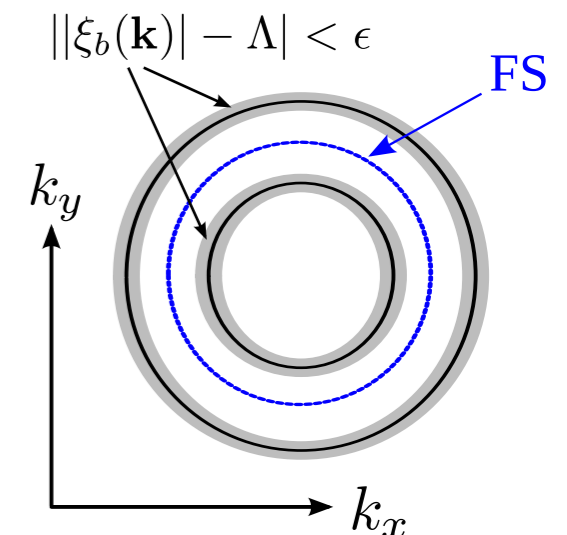
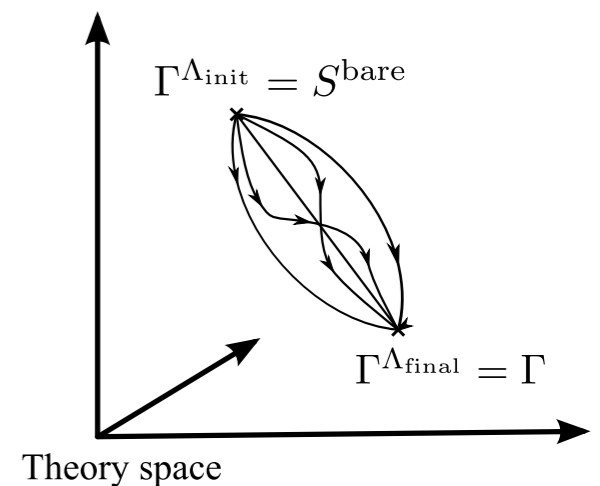
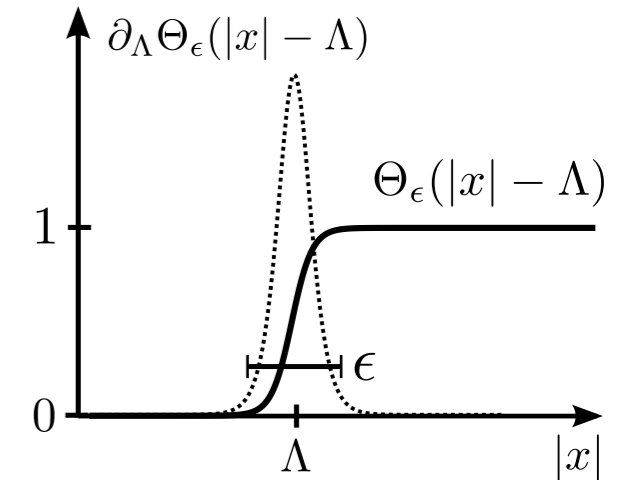
→ variation w.r.t to scale provides **exact RG equation**:

$$\frac{\partial}{\partial \Lambda} \Gamma^\Lambda[\phi, \bar{\phi}] = \text{Tr} \left[G_0^\Lambda \frac{\partial (G_0^\Lambda)^{-1}}{\partial \Lambda} \right] - \text{Tr} \left[\left(\frac{\delta^2 \Gamma^\Lambda[\phi, \bar{\phi}]}{\delta \phi \delta \bar{\phi}} + (G_0^\Lambda)^{-1} \right)^{-1} \frac{\partial (G_0^\Lambda)^{-1}}{\partial \Lambda} \right]$$

 Wetterich (1993)

 Salmhofer & Honerkamp (2001)

- ▶ exact RG equation has one-loop structure
- ▶ removing cutoff ($\Lambda \rightarrow 0$) yields the full effective action
- ▶ lowering cutoff corresponds to momentum-shell integration



 from Platt, Hanke, Thomale (2013)

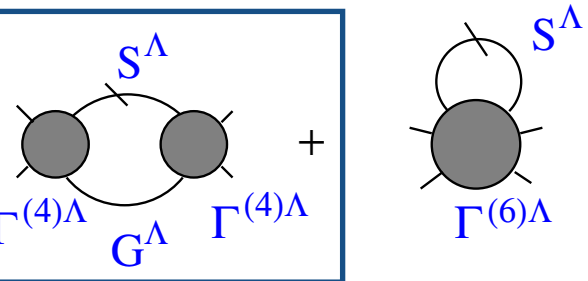
Truncation and approximations

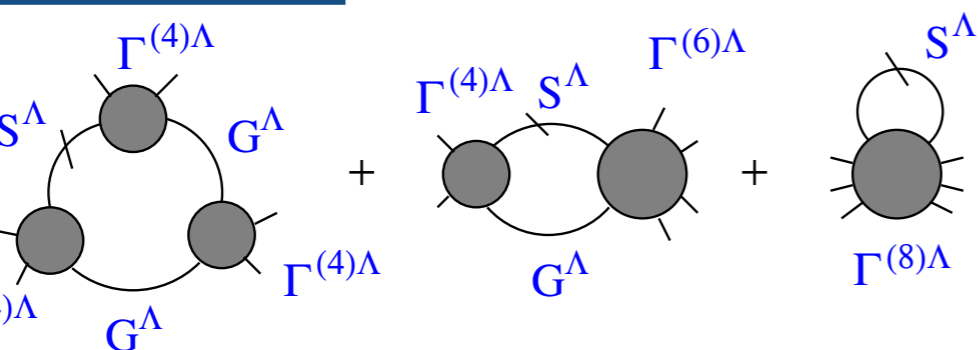
- ▶ exact RG equation cannot be solved exactly!
- ▶ starting point for systematic approximations (vertex expansion)

$$\Gamma^\Lambda[\phi, \bar{\phi}] = \sum_{m=0}^{\infty} \frac{1}{(m!)^2} \sum_{K_1 \dots K_m} \sum_{K'_1 \dots K'_m} \gamma_m^\Lambda(K'_1, \dots, K'_m; K_1, \dots, K_m) \prod_{j=1}^m \bar{\phi}_{K'_j} \phi_{K_j}$$

$\frac{d}{d\Lambda} \Sigma^\Lambda =$  $\Gamma^{(4)\Lambda}$

exact RG equation

$$\frac{d}{d\Lambda} \Gamma^{(4)\Lambda} =$$


$$\frac{d}{d\Lambda} \Gamma^{(6)\Lambda} =$$


- ▶ neglect 6-point and higher vertices
- ▶ neglect self-energy feedback

 Salmhofer & Honerkamp (2001)

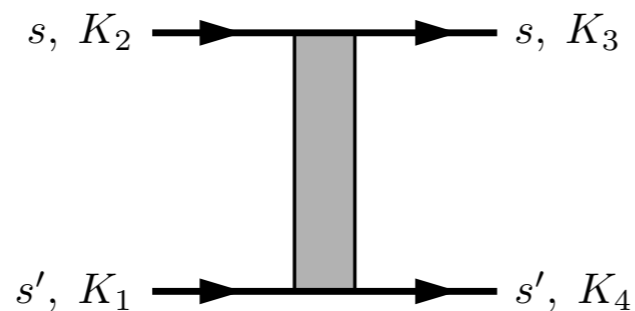
... infinite hierarchy of flow equations!

Symmetries and approximations

▶ system with **spin-rotational invariance**:

- RG flow of general 4-point function $\Gamma^{(4)\Lambda}$: $\Gamma_{\sigma_1, \sigma_2, \sigma_3, \sigma_4}^{(4)\Lambda} = V^\Lambda \delta_{\sigma_1 \sigma_3} \delta_{\sigma_2 \sigma_4} - V^\Lambda \delta_{\sigma_1 \sigma_4} \delta_{\sigma_2 \sigma_3}$

➔ **interaction vertex V^Λ** :



$$V_\Lambda(k_1, k_2, k_3, k_4)$$

- ▶ momentum arguments include *frequency, wavevector* and *orbital* indices
- ▶ ground-state properties: neglect frequency dependence, set external frequencies to zero

Symmetries and approximations

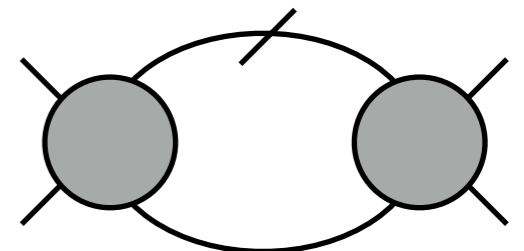
▶ system with **spin-rotational invariance**:

- RG flow of general 4-point function $\Gamma^{(4)\Lambda}$: $\Gamma_{\sigma_1, \sigma_2, \sigma_3, \sigma_4}^{(4)\Lambda} = V^\Lambda \delta_{\sigma_1 \sigma_3} \delta_{\sigma_2 \sigma_4} - V^\Lambda \delta_{\sigma_1 \sigma_4} \delta_{\sigma_2 \sigma_3}$

➔ flow of **spin-independent interaction vertex V^Λ** :

$$\begin{aligned} \frac{d}{d\Lambda} V^\Lambda(K_1, K_2; K_3, K_4) = & \int dK V^\Lambda(K_1, K_2, K) L^\Lambda(K, -K + K_1 + K_2) V^\Lambda(K, -K + K_1 + K_2, K_3), \\ & + \int dK \left[-2V^\Lambda(K_1, K, K_3) L^\Lambda(K, K + K_1 - K_3) V^\Lambda(K + K_1 - K_3, K_2, K) \right. \\ & \quad + V^\Lambda(K_1, K, K + K_1 - K_3) L^\Lambda(K, K + K_1 - K_3) V^\Lambda(K + K_1 - K_3, K_2, K) \\ & \quad \left. + V^\Lambda(K_1, K, K_3) L^\Lambda(K, K + K_1 - K_3) V^\Lambda(K_2, K + K_1 - K_3, K) \right], \\ & + \int dK V^\Lambda(K_1, K + K_2 - K_3, K) L^\Lambda(K, K + K_2 - K_3) V^\Lambda(K, K_2, K_3). \end{aligned}$$

- where $L^\Lambda(K, K') = \frac{d}{d\Lambda} [G_0^\Lambda(K) G_0^\Lambda(K')]$



Symmetries and approximations

▶ system with **spin-rotational invariance**:

- RG flow of general 4-point function $\Gamma^{(4)\Lambda}$: $\Gamma_{\sigma_1, \sigma_2, \sigma_3, \sigma_4}^{(4)\Lambda} = V^\Lambda \delta_{\sigma_1 \sigma_3} \delta_{\sigma_2 \sigma_4} - V^\Lambda \delta_{\sigma_1 \sigma_4} \delta_{\sigma_2 \sigma_3}$

➔ flow of **spin-independent interaction vertex V^Λ** :

$$\frac{d}{d\Lambda} V^\Lambda(K_1, K_2; K_3, K_4) =$$

Cooper
Peierls
Screening
Vertex corrections
Vertex corrections

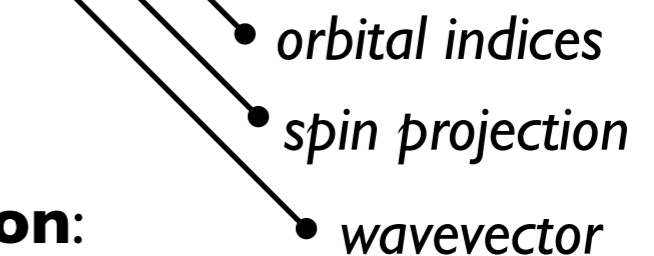
- corresponds to *infinite order summation* of one-loop *pp* and *ph* terms
- unbiased investigation of competition between various correlations
- **flow to strong coupling** indicates **ordering transition**: analyze components of V^Λ

Multi-orbital models

► **orbital degrees of freedom:**

- valley d.o.f. in tBLG, d -orbitals of iron pnictides and transition-metal oxides
- sublattice index of bipartite/multi-layer lattice (e.g., graphene's honeycomb lattice)

- general non-interacting part of multi-orbital model: $H_0 = \sum_{\vec{k},s} \sum_{o,o'} c_{o,s,\vec{k}}^\dagger K_{o,o'}(\vec{k}) c_{o',s,\vec{k}}$



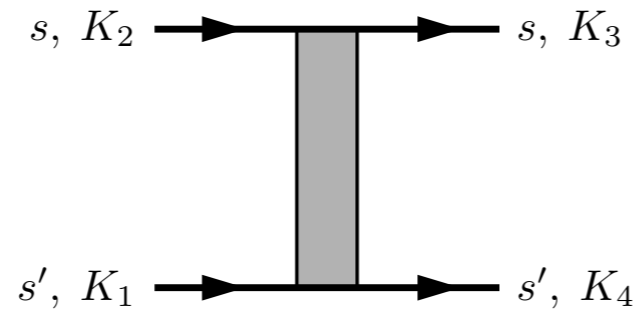
- unitary transformation to **energy band representation:**

$$\begin{aligned}
 c_{b,s,\vec{k}} &= \sum_o u_{bo,\vec{k}} c_{o,s,\vec{k}} \\
 c_{b,s,\vec{k}}^\dagger &= \sum_o u_{bo,\vec{k}}^* c_{o,s,\vec{k}}^\dagger
 \end{aligned}
 \quad \Rightarrow \quad
 H_0 = \sum_{\vec{k},s,b} E_b(\vec{k}) c_{b,s,\vec{k}}^\dagger c_{b,s,\vec{k}}$$

- interaction part of Hamiltonian has to be transformed accordingly

➡ adds momentum dependence to interaction vertex at bare level - **orbital makeup**

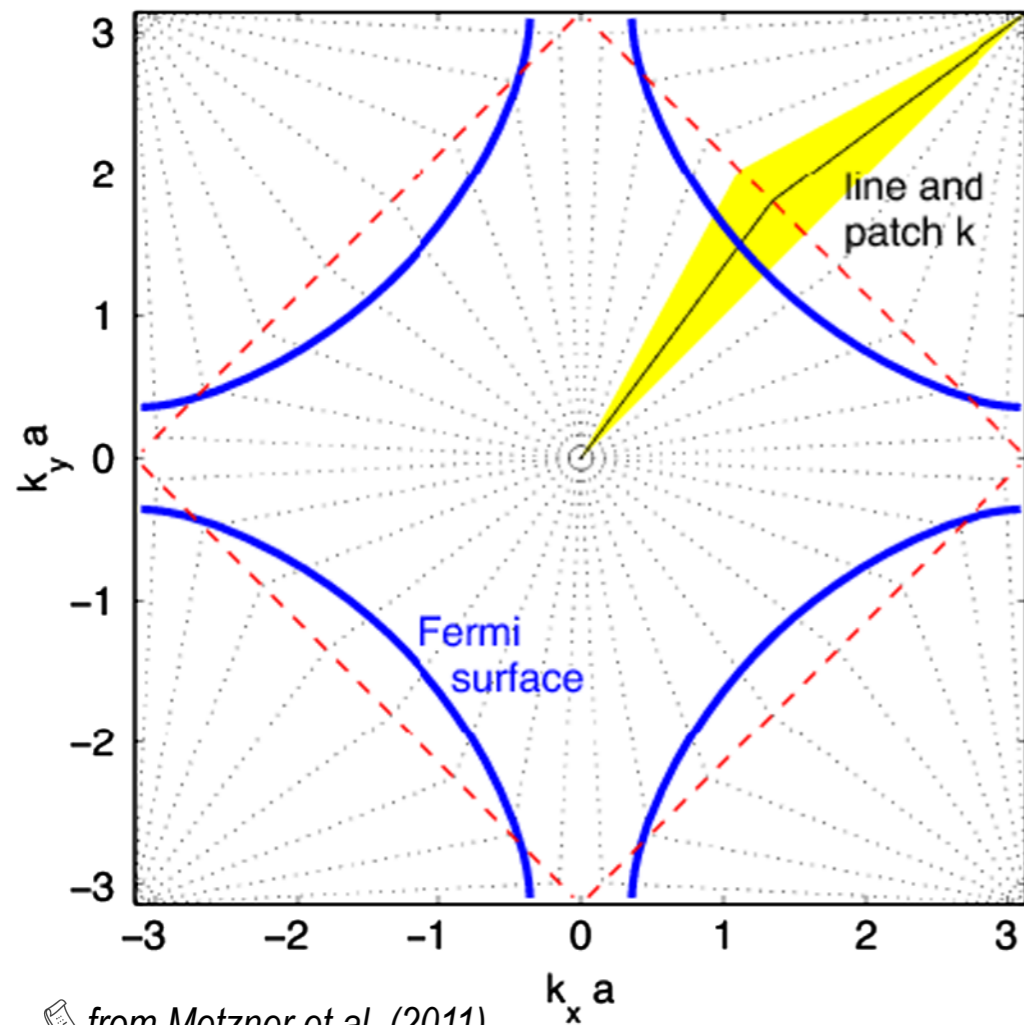
Fermi-surface patching scheme



$$V_{\Lambda}(k_1, k_2, k_3, k_4)$$

- ▶ wavevector dependence of **Fermi surface** from discretization in **N patches**:

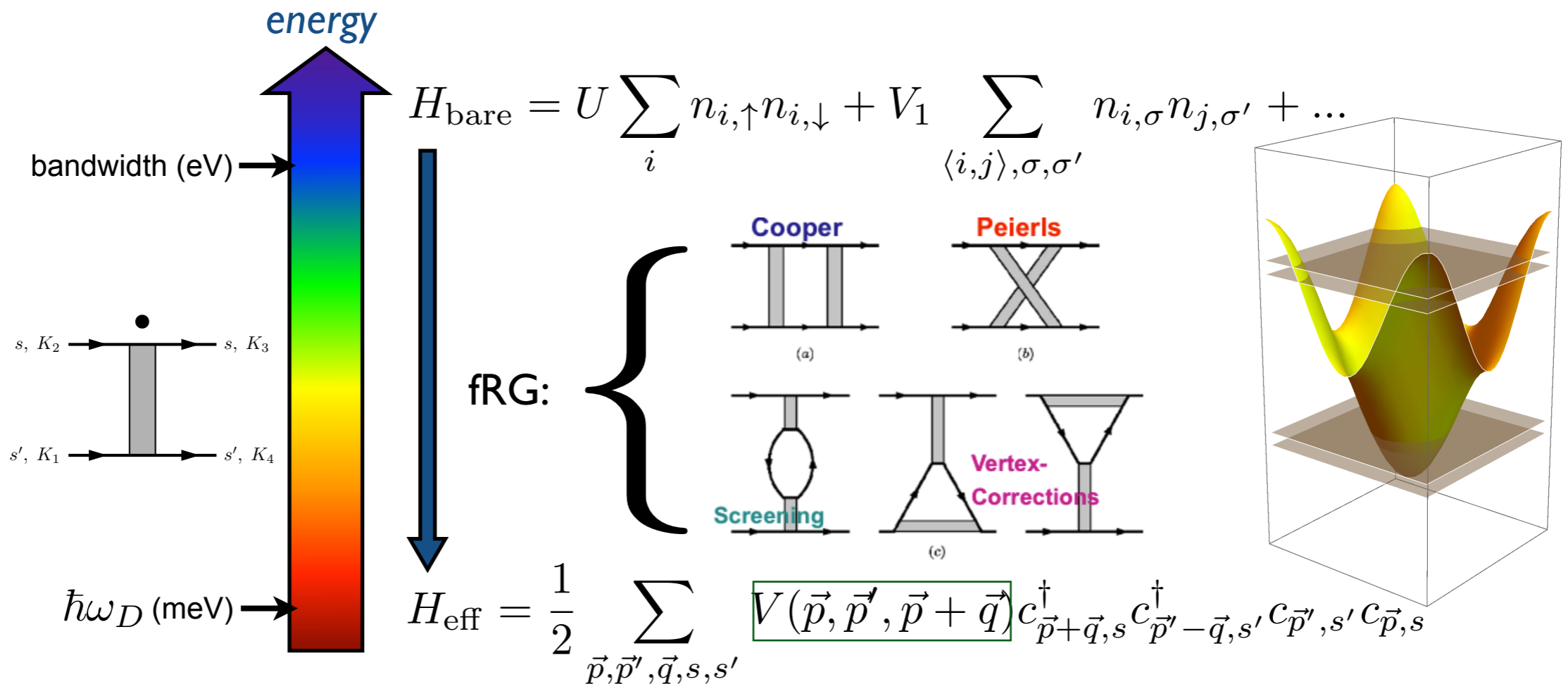
$N=32$



- ▶ **interaction constant within one patch**
- ▶ representative momenta lie at Fermi level
- ▶ **finite set of coupled flow equations** for components of V^{Λ}
- ▶ facilitates numerical implementation
- ▶ **example:**
 - t - t' - μ -Hubbard model on the square lattice: vertex has N^3 components
 - generally: V^{Λ} has $N_b^4 N^3$ components

fRG: from **bare** to **effective** interaction

- ▶ excitations at intermediate scales generate momentum structure in low-energy interaction



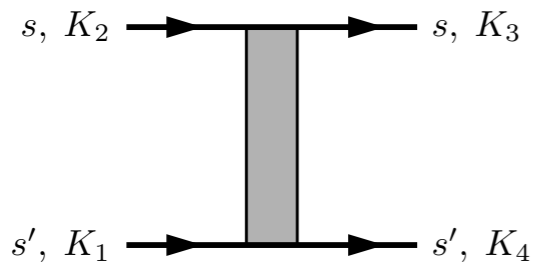
- ▶ low-energy effective action & momentum structure

➔ two-particle interaction vertex $V(\vec{p}, \vec{p}', \vec{p} + \vec{q})$

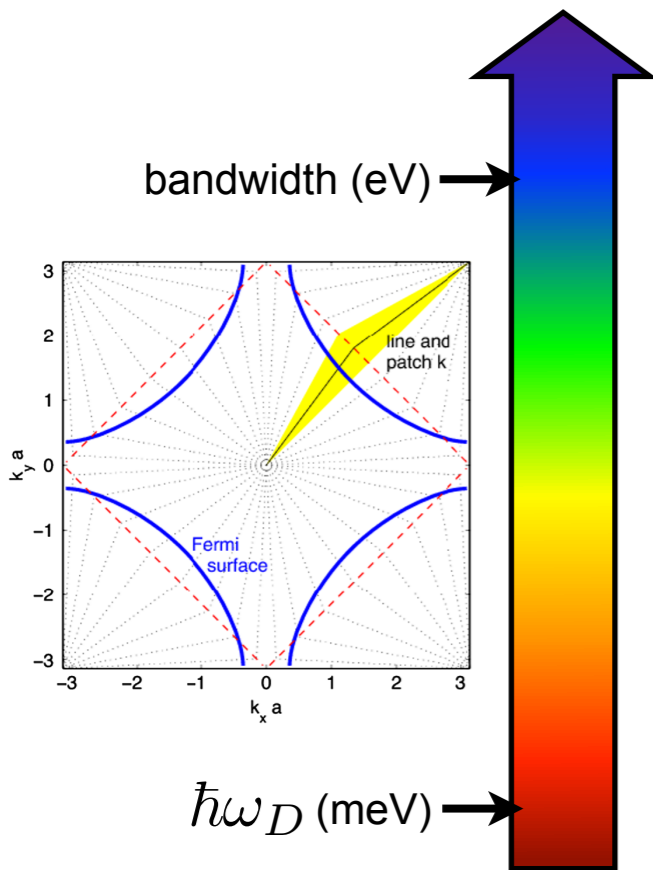
➔ flow to strong coupling: singularity for $\Lambda \rightarrow \Lambda^*$

➔ read off dominant interactions and e.g. extract form factors of order parameters

fRG: from **bare** to **effective interaction**

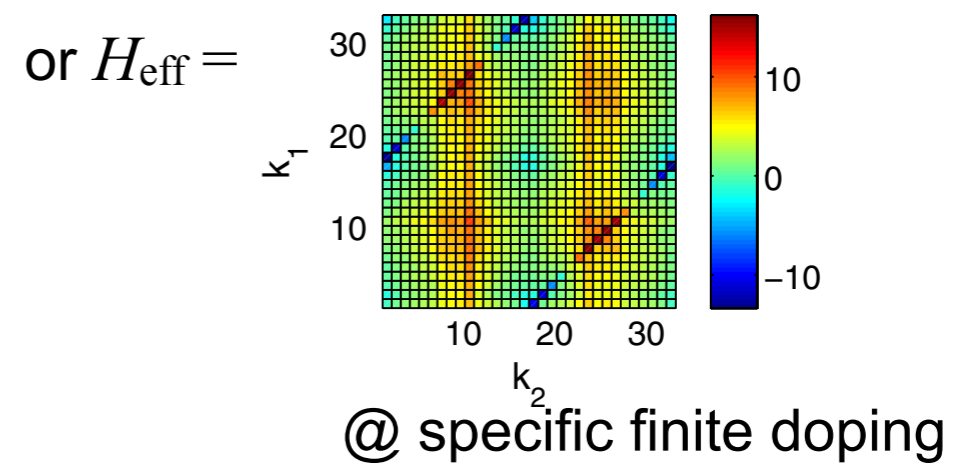
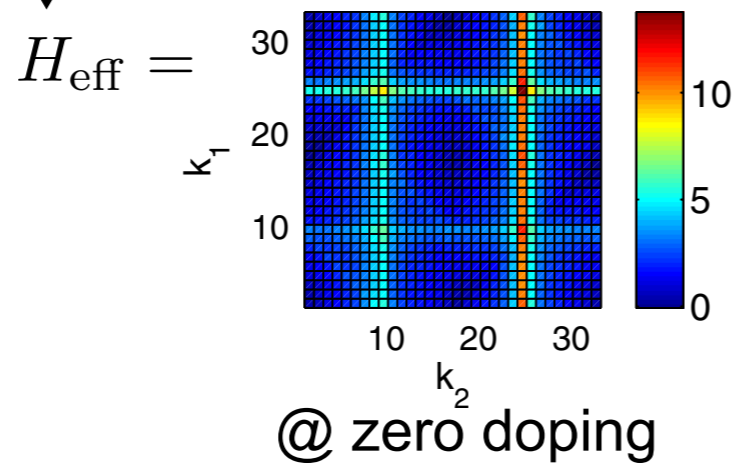
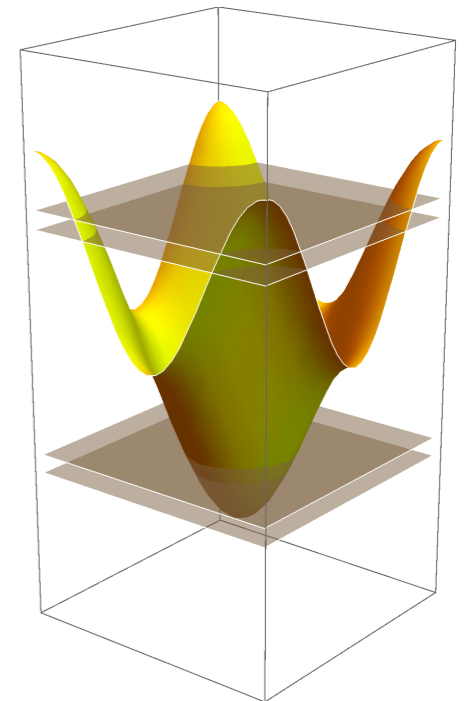
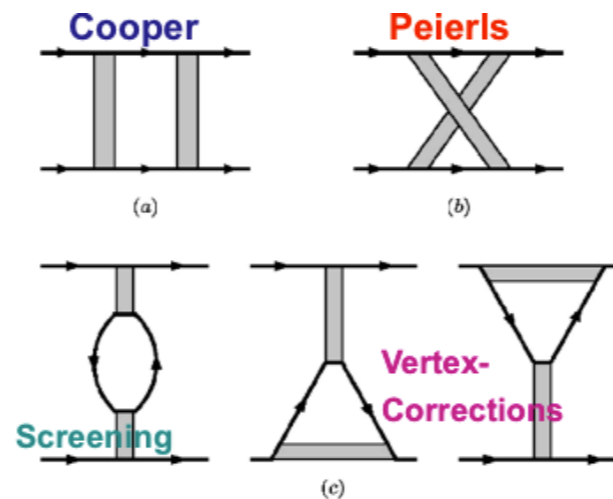


- ▶ sharp momentum structures in the interaction vertex emerge
- ▶ e.g., onsite interaction ($U=3.0t$), typical pattern (k_3 fixed at point 1):



$$H_{\text{bare}} = U \sum_i n_{i,\uparrow} n_{i,\downarrow}$$

fRG:



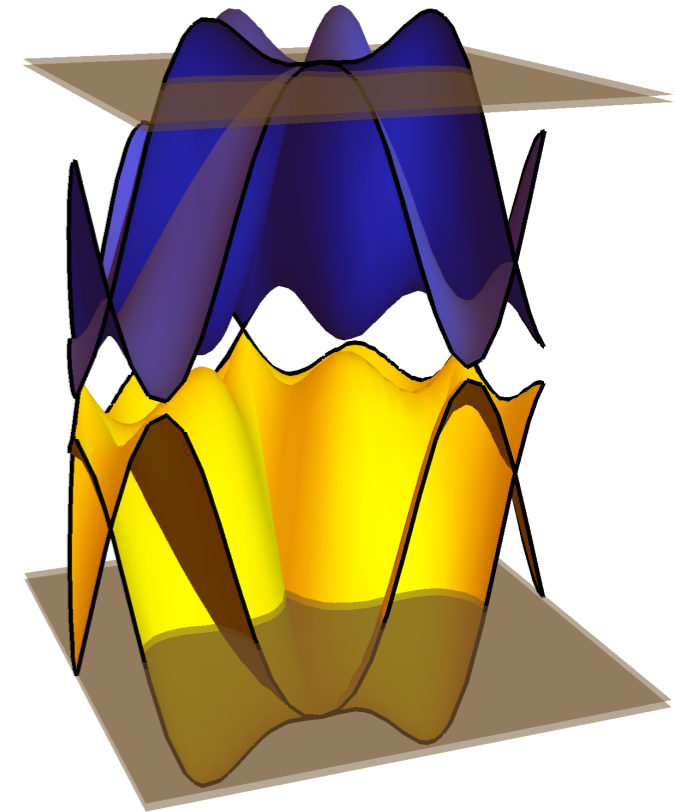
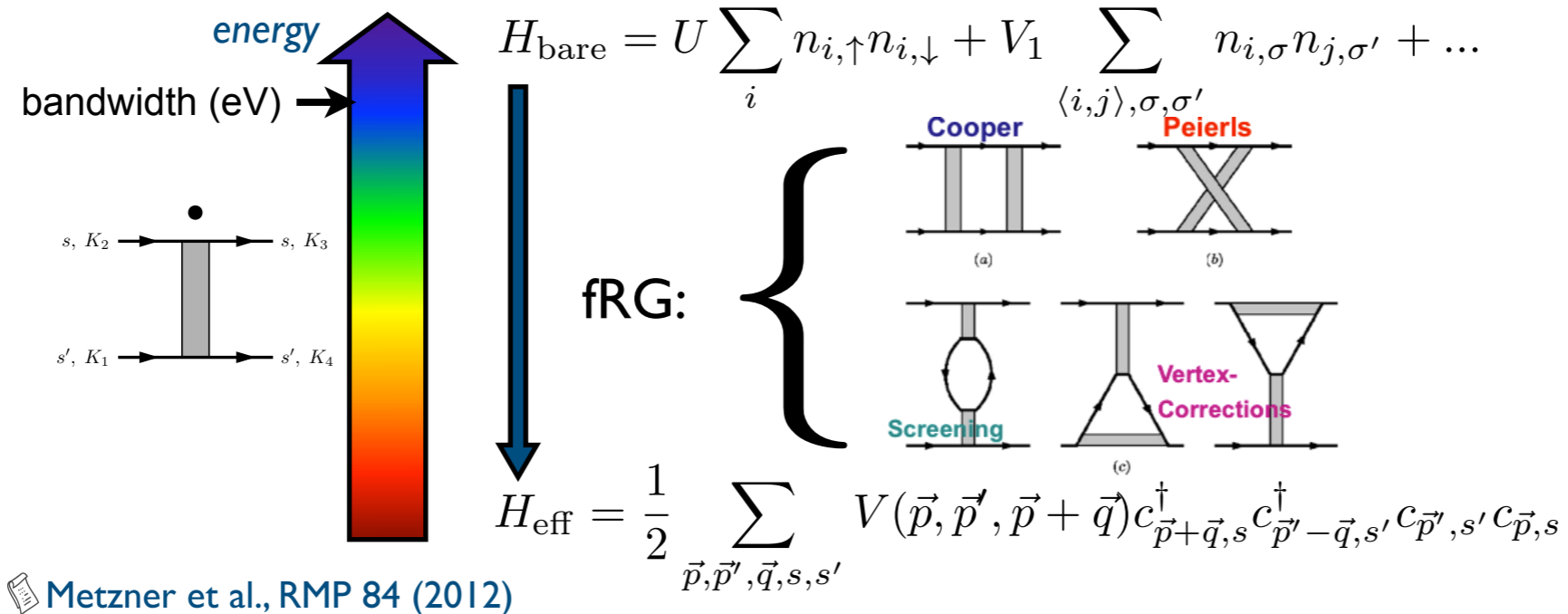
$$J \sum_{\langle i,j \rangle} e^{i\mathbf{Q} \cdot (\mathbf{R}_i - \mathbf{R}_j)} \mathbf{S}_i \cdot \mathbf{S}_j$$

$$H_{\text{dSC}}^\Lambda = V_{\text{dSC}} \sum_{\mathbf{k}, \mathbf{k}'} d(\mathbf{k}) d(\mathbf{k}') c_{\mathbf{k}', \uparrow}^\dagger c_{-\mathbf{k}', \downarrow}^\dagger c_{-\mathbf{k}, \downarrow} c_{\mathbf{k}, \uparrow}$$

- ▶ mean-field decoupling \rightarrow antiferromagnetic SDW (**AF-SDW**) or **d-wave SC**

fermion fRG approach — Precis

- *fermion fRG*: discovery tool for leading many-body instabilities



- treats all fermionic fluctuation channels on *equal footing*
- *infinite-order resummation* of all fermionic 1-loop diagrams
- can deal with *multi-orbital band structures, non-local i.a. & competing correlations*
- due to truncations/approximations: **qualitative** (not quantitative) tool
- *prediction* of different types of *magnetism / superconductivity / bond order states / ...*

Minimal phenomenological model for tDBLG

1. *triangular* lattice near van-Hove filling (twisted **double** bilayer graphene)
2. weak tunnelling between nearest-neighbor unit supercells dominates kinetic energy
3. each cell hosts two degenerate orbitals from original valleys +/-
4. no mixing of orbitals due to large momentum space separation
5. spin-independent hopping of electrons

 Balents & Xu, PRL 121, 087001 (2018)

 **two-orbital tight-binding model** $H_{\text{kin}} = -t \sum_{\langle ij \rangle} \sum_{\sigma=\uparrow,\downarrow} \sum_{o=\pm} \left(c_{i\sigma o}^\dagger c_{j\sigma o} + \text{h.c.} \right)$

- 4 flavours: $\alpha \in \{(\uparrow,+), (\downarrow,+), (\uparrow,-), (\downarrow,-)\} \rightarrow$ effective SU(4) symmetry
- add SU(4) symmetric Hubbard interaction as minimal interaction

$$H_{\text{int}} = U \sum_i \left(\sum_{\alpha=1}^4 n_{i\alpha} \right)^2$$

- dominant interaction depends only on total charge of site

Next-to-minimal model

- Include **Hund's couplings**: $H_h = -V_h \sum_i \vec{S}_i \cdot \vec{S}_i$

- with $\vec{S}_i = \frac{1}{2} c_{i\sigma o}^\dagger \vec{\sigma}_{\sigma\sigma'} c_{i\sigma' o}$

- breaks SU(4)

- alternatively “orbital” Hund's coupling (**anti-Hund**):

$$H_K = -K \sum_i \vec{L}_i \cdot \vec{L}_i \quad \text{with} \quad \vec{L}_i = \frac{1}{2} c_{i\sigma o}^\dagger \vec{\tau}_{oo'} c_{i\sigma o'}$$

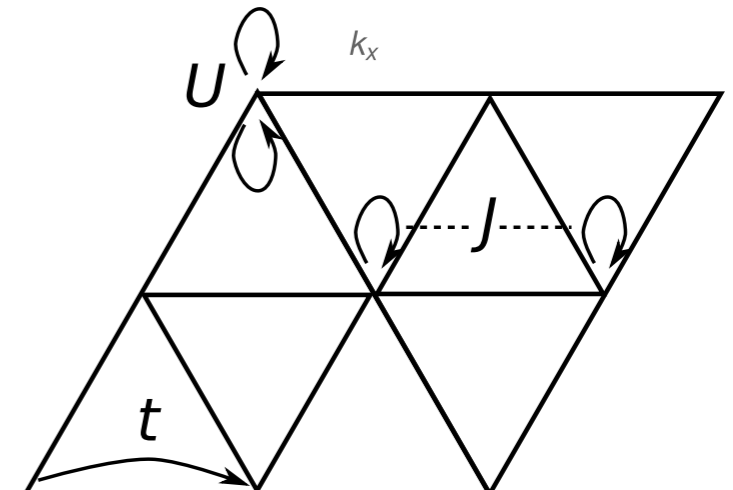
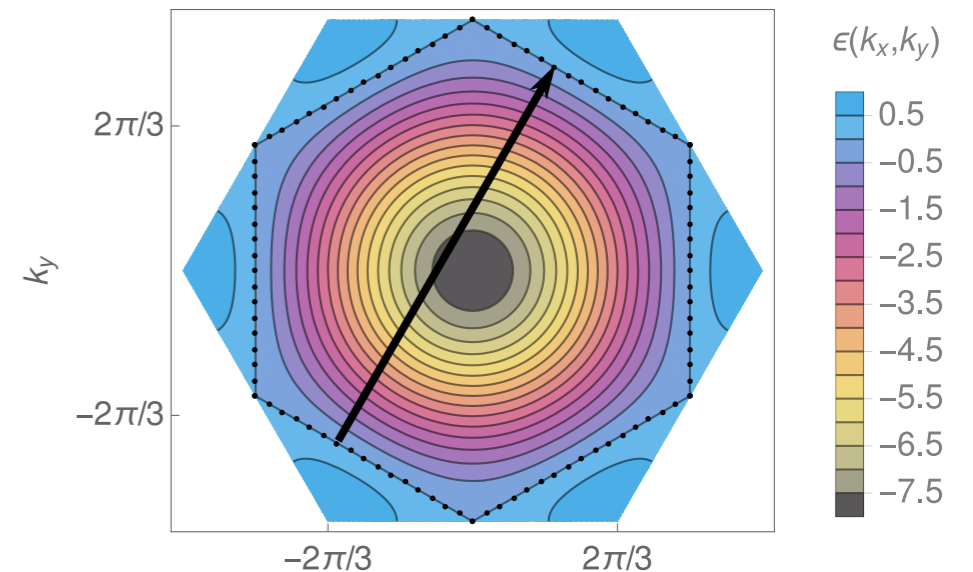
- also add SU(4) **exchange coupling** J

- **hierarchy of model parameters**:

- strong onsite interaction $U > J, V_h,$
- approximate SU(4): $U > V_h, K$
- tune filling by chemical potential μ

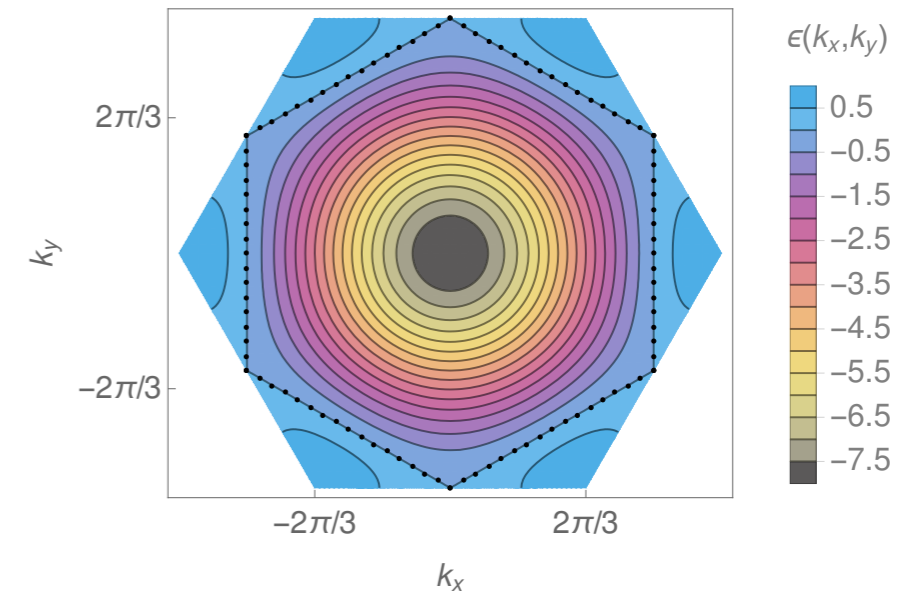
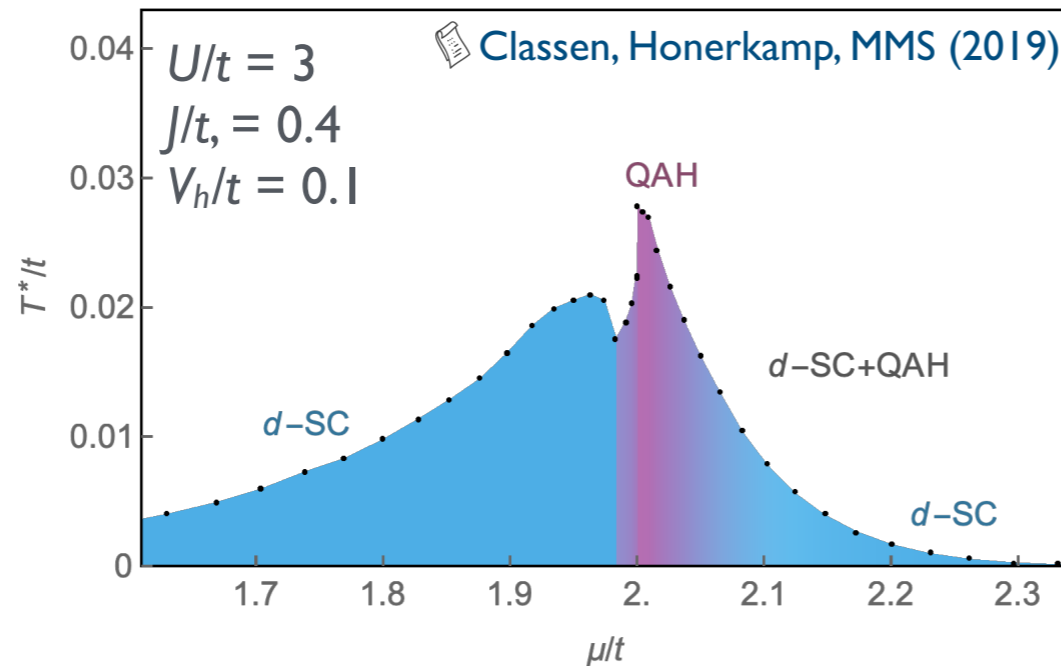
➡ **fRG phase diagram...**

- Xu & Balents
- Dodaro, Kivelson, Schattner, Sun, Wang
- Yuan & Fu
- Po, Zou, Vishwanath, Senthil



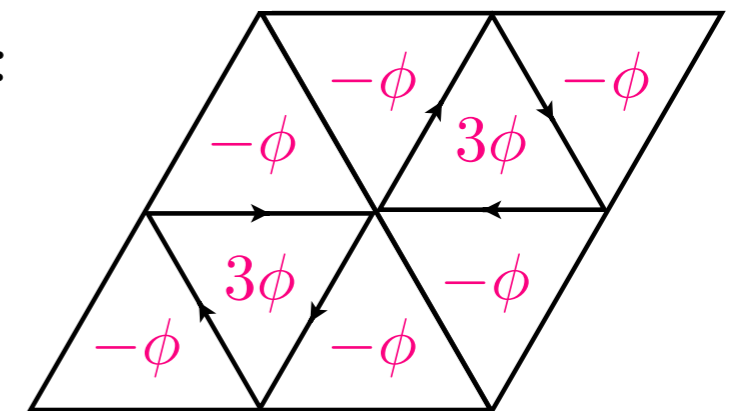
Next-to-minimal models — functional RG approach

- *phase diagram:*



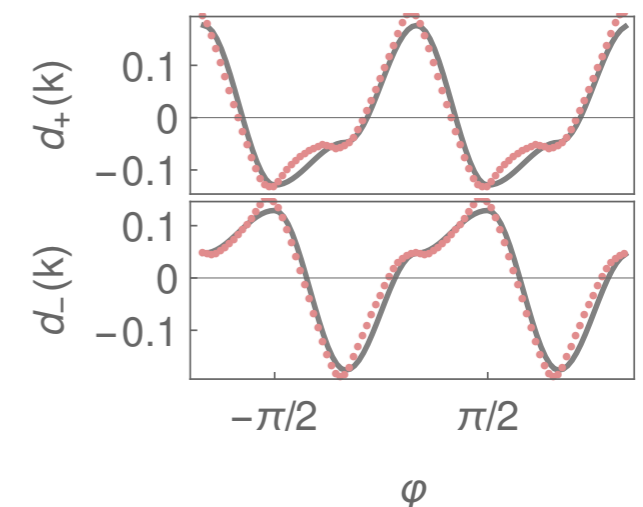
- **interaction-induced quantum anomalous Hall state:**

- robust near van-Hove filling, fully gapped spectrum
- breaks time-reversal symmetry
- Chern insulator: Haldane-like loop current



- **$d \pm id$ superconductivity:**

- SC form factor superposition of $d_{xy}(k)$ and $d_{x^2-y^2}(k)$
- expect lowest energy for full gap $\rightarrow d_{xy} \pm id_{x^2-y^2}$ superposition
- for $V_h > K$: (spin-singlet) \times (orbital-triblet) pairing function



...next: **implementation of realistic lattice models...**

Conclusions & Outlook

Conclusions and Outlook

- Superlattice modulation of moiré heterostructures
 - flat bands, strongly-correlated physics, “high- T_c ” phase diagrams, highly tunable
- **Open questions**
 - appropriate models and characterization of correlated states
 - weak-coupling vs. strong coupling perspective
- Competing orders/instabilities → **fermion fRG** (for tdBLG)

- next-to-minimal triangular $SU(2) \times SU(2)$

- main phases:

-  Chern insulating **QAH** state

-  **$d \pm id$** superconductivity

